

FATIGUE, CREEP AND FRACTURE**Summary**

Fatigue loading is generally defined by the following parameters

$$\text{stress range, } \sigma_r = 2\sigma_a$$

$$\text{mean stress, } \sigma_m = \frac{1}{2}(\sigma_{\max} + \sigma_{\min})$$

$$\text{alternating stress amplitude, } \sigma_a = \frac{1}{2}(\sigma_{\max} - \sigma_{\min})$$

When the mean stress is not zero

$$\text{stress ratio, } R_s = \frac{\sigma_{\min}}{\sigma_{\max}}$$

The *fatigue strength* σ_N for N cycles under zero mean stress is related to that σ_a under a condition of mean stress σ_m by the following alternative formulae:

$$\sigma_a = \sigma_N [1 - (\sigma_m / \sigma_{TS})] \quad (\text{Goodman})$$

$$\sigma_a = \sigma_N [1 - (\sigma_m / \sigma_{TS})^2] \quad (\text{Geber})$$

$$\sigma_a = \sigma_N [1 - (\sigma_m / \sigma_y)] \quad (\text{Soderberg})$$

where σ_{TS} = tensile strength and σ_y = yield strength of the material concerned. Applying a factor of safety F to the Soderberg relationship gives

$$\sigma_a = \frac{\sigma_N}{F} \left[1 - \left(\frac{\sigma_m \cdot F}{\sigma_y} \right) \right]$$

Theoretical elastic stress concentration factor for elliptical crack of major and minor axes A and B is

$$K_t = 1 + 2A/B$$

The relationship between any given number of cycles n at one particular stress level to that required to break the component at the same stress level N is termed the “*stress ratio*” (n/N). *Miner’s law* then states that for cumulative damage actions at various stress levels:

$$\frac{n_1}{N_1} + \frac{n_2}{N_2} + \frac{n_3}{N_3} + \dots + \text{etc.} = 1$$

The *Coffin–Manson law* relating the plastic strain range $\Delta \varepsilon_p$ to the number of cycles to failure N_f is:

$$\Delta \varepsilon_p = K(N_f)^{-b}$$

or

$$\Delta \varepsilon_p = \left(\frac{N_f}{D} \right)^{-b}$$

where D is the ductility, defined in terms of the reduction in area r during a tensile test as

$$D = l_n \left(\frac{1}{1-r} \right)$$

The total strain range = elastic + plastic strain ranges

i.e.
$$\Delta \varepsilon_t = \Delta \varepsilon_e + \Delta \varepsilon_p$$

the elastic range being given by *Basquin's law*

$$\Delta \varepsilon_e = \frac{3.5 \sigma_{TS}}{E} \cdot N_f^{-0.12}$$

Under creep conditions the *secondary creep rate* ε_s^0 is given by the *Arrhenius equation*

$$\varepsilon_s^0 = A e^{\left(-\frac{H}{RT} \right)}$$

where H is the activation energy, R the universal gas constant, T the absolute temperature and A a constant.

Under increasing stress the power law equation gives the secondary creep rate as

$$\varepsilon_s^0 = \beta \sigma^n$$

with β and n both being constants.

The latter two equations can then be combined to give

$$\varepsilon_s^0 = K \sigma^n e^{\left(-\frac{H}{RT} \right)}$$

The *Larson–Miller parameter* for life prediction under creep conditions is

$$P_1 = T(\log_{10} t_r + C)$$

The *Sherby–Dorn parameter* is

$$P_2 = \log_{10} t_r - \frac{\alpha}{T}$$

and the *Manson–Haferd parameter*

$$P_3 = \frac{T - T_a}{\log_{10} t_r - \log_{10} t_a}$$

where t_r = time to rupture and T_a and $\log_{10} t_a$ are the coordinates of the point at which graphs of T against $\log_{10} t_r$ converge. C and α are constants.

For stress relaxation under constant strain

$$\frac{1}{\sigma^{n-1}} = \frac{1}{\sigma_i^{n-1}} + \beta E(n-1)t$$

where σ is the instantaneous stress, σ_i the initial stress, β and n the constants of the power law equation, E is Young's modulus and t the time interval.

Griffith predicts that fracture will occur at a fracture stress σ_f given by

$$\sigma_f^2 = \frac{2bE\gamma}{\pi a(1-\nu^2)} \quad \text{for plane strain}$$

or
$$\sigma_f^2 = \frac{2bE\gamma}{\pi a} \quad \text{for plane stress}$$

where $2a$ = initial crack length (in an infinite sheet)

b = sheet thickness

γ = surface energy of crack faces.

Irwin's expressions for the cartesian components of stress at a crack tip are, in terms of polar coordinates;

$$\sigma_{yy} = \frac{K}{\sqrt{2\pi r}} \cos \frac{\theta}{2} \left[1 + \sin \frac{\theta}{2} \sin \frac{3\theta}{2} \right]$$

$$\sigma_{xx} = \frac{K}{\sqrt{2\pi r}} \cos \frac{\theta}{2} \left[1 - \sin \frac{\theta}{2} \sin \frac{3\theta}{2} \right]$$

$$\sigma_{xy} = \frac{K}{\sqrt{2\pi r}} \cos \frac{\theta}{2} \sin \frac{\theta}{2} \cos \frac{3\theta}{2}$$

where K is the stress intensity factor = $\sigma\sqrt{\pi a}$

or, for an edge-crack in a semi-infinite sheet

$$K = 1.12\sigma\sqrt{\pi a}$$

For finite size components with cracks generally growing from a free surface the stress intensity factor is modified to

$$K = \sigma Y \sqrt{a}$$

where Y is a compliance function of the form

$$Y = A \left(\frac{a}{W} \right)^{1/2} - B \left(\frac{a}{W} \right)^{3/2} + C \left(\frac{a}{W} \right)^{5/2} - D \left(\frac{a}{W} \right)^{7/2} + E \left(\frac{a}{W} \right)^{9/2}$$

In terms of load P , thickness b and width W

$$K = \frac{P}{bW^{1/2}} \cdot Y$$

For elastic-plastic conditions the plastic zone size is given by

$$r_p = \frac{K^2}{\pi\sigma_y^2} \quad \text{for plane stress}$$

and

$$r_p = \frac{K^2}{3\pi\sigma_y^2} \quad \text{for plane strain}$$

r_p being the extent of the plastic zone along the crack axis measured from the crack tip.

Mode II crack growth is described by the Paris-Erdogan Law

$$\frac{da}{dN} = C(\Delta K)^m$$

where C and m are material coefficients.

11.1. Fatigue

Introduction

Fracture of components due to fatigue is the most common cause of service failure, particularly in shafts, axles, aircraft wings, etc., where cyclic stressing is taking place. With static loading of a ductile material, plastic flow precedes final fracture, the specimen necks and the fractured surface reveals a fibrous structure, but with fatigue, the crack is initiated from points of high stress concentration on the surface of the component such as sharp changes in cross-section, slag inclusions, tool marks, etc., and then spreads or propagates under the influence of the load cycles until it reaches a critical size when fast fracture of the remaining cross-section takes place. The surface of a typical fatigue-failed component shows three areas, the small point of initiation and then, spreading out from this point, a smaller glass-like area containing shell-like markings called “*arrest lines*” or “*conchoidal markings*” and, finally, the crystalline area of rupture.

Fatigue failures can and often do occur under loading conditions where the fluctuating stress is below the tensile strength and, in some materials, even below the elastic limit. Because of its importance, the subject has been extensively researched over the last one hundred years but even today one still occasionally hears of a disaster in which fatigue is a prime contributing factor.

11.1.1. The S/N curve

Fatigue tests are usually carried out under conditions of rotating – bending and with a zero mean stress as obtained by means of a Wohler machine.

From Fig. 11.1, it can be seen that the top surface of the specimen, held “cantilever fashion” in the machine, is in tension, whilst the bottom surface is in compression. As the specimen rotates, the top surface moves to the bottom and hence each segment of the surface moves continuously from tension to compression producing a stress-cycle curve as shown in Fig. 11.2.

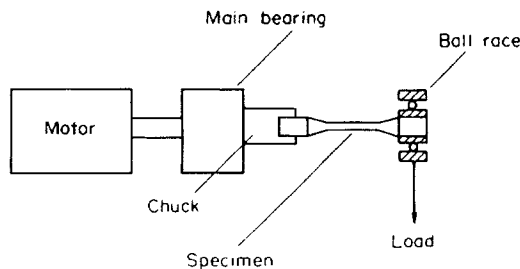


Fig. 11.1. Single point load arrangement in a Wohler machine for zero mean stress fatigue testing.

In order to understand certain terms in common usage, let us consider a stress-cycle curve where there is a positive tensile mean stress as may be obtained using other types of fatigue machines such as a Haigh “push-pull” machine.

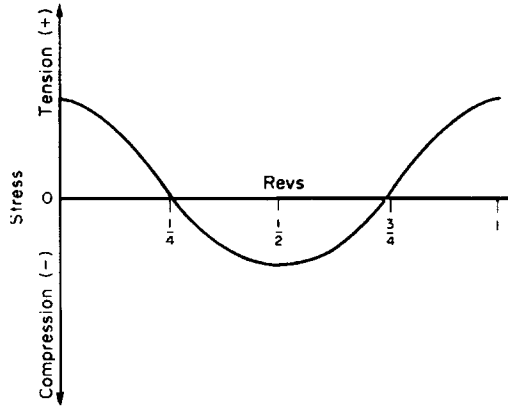


Fig. 11.2. Simple sinusoidal (zero mean) stress fatigue curve, “reversed-symmetrical”.

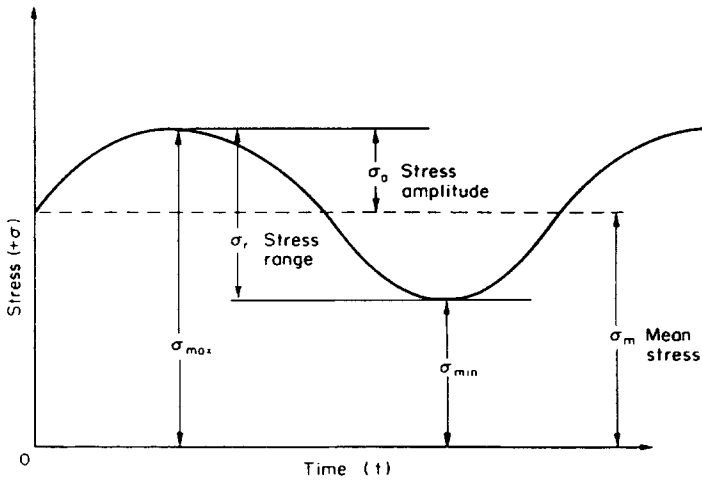


Fig. 11.3. Fluctuating tension stress cycle producing positive mean stress.

The stress-cycle curve is shown in Fig. 11.3, and from this diagram it can be seen that:

$$\text{Stress range, } \sigma_r = 2\sigma_a. \tag{11.1}$$

$$\text{Mean stress, } \sigma_m = \frac{\sigma_{\max} + \sigma_{\min}}{2} \tag{11.2}$$

$$\text{Alternating stress amplitude, } \sigma_a = \frac{\sigma_{\max} - \sigma_{\min}}{2} \tag{11.3}$$

If the mean stress is not zero, we sometimes make use of the “stress ratio” R_s , where

$$R_s = \frac{\sigma_{\min}}{\sigma_{\max}} \tag{11.4}$$

The most general method of presenting the results of a fatigue test is to plot a graph of the stress amplitude as ordinate against the corresponding number of cycles to failure as

abscissa, the amplitude being varied for each new specimen until sufficient data have been obtained. This results in the production of the well-known S/N curve – Fig. 11.4.

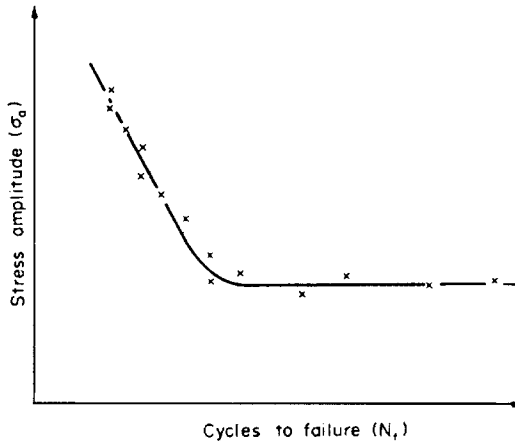


Fig. 11.4. Typical S/N curve fatigue life curve.

In using the S/N curve for design purposes it may be advantageous to express the relationship between σ_a and N_f , the number of cycles to failure. Various empirical relationships have been proposed but, provided the stress applied does not produce plastic deformation, the following relationship is most often used:

$$\sigma_r^a N_f = K \quad (11.5)$$

Where a is a constant which varies from 8 to 15 and K is a second constant depending on the material – see Example 11.1.

From the S/N curve the “fatigue limit” or “endurance limit” may be ascertained. The “*fatigue limit*” is the stress condition below which a material may endure an infinite number of cycles prior to failure. Ferrous metal specimens often produce S/N curves which exhibit fatigue limits as indicated in Fig. 11.5(a). The “*fatigue strength*” or “*endurance limit*”, is the stress condition under which a specimen would have a fatigue life of N cycles as shown in

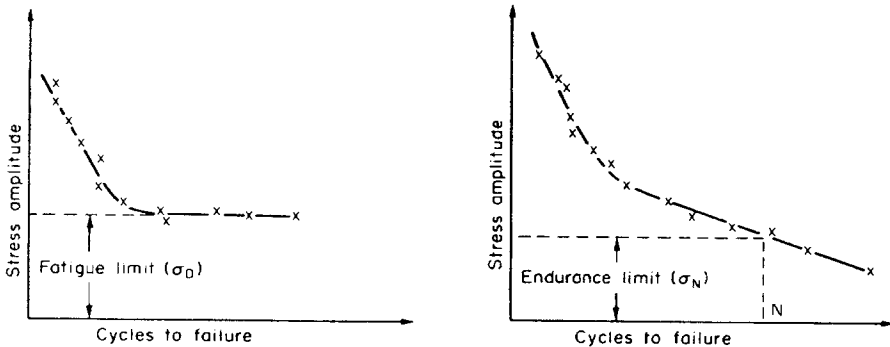


Fig. 11.5. S/N curve showing (a) fatigue limit, (b) endurance limit.

Fig. 10.5(b). Non-ferrous metal specimens show this type of curve and hence components made from aluminium, copper and nickel, etc., must always be designed for a finite life.

Another important fact to note is that the results of laboratory experiments utilising plain, polished, test pieces cannot be applied directly to structures and components without modification of the intrinsic values obtained. Allowance will have to be made for many differences between the component in its working environment and in the laboratory test such as the surface finish, size, type of loading and effect of stress concentrations. These factors will reduce the intrinsic (i.e. plain specimen) fatigue strength value thus,

$$\sigma'_N = \frac{\sigma_N}{K_f} [C_a \cdot C_b \cdot C_c] \quad (11.6)$$

where σ'_N is the “modified fatigue strength” or “modified fatigue limit”, σ_N is the intrinsic value, K_f is the fatigue strength reduction factor (see § 11.1.4) and C_a , C_b and C_c are factors allowing for size, surface finish, type of loading, etc.

The types of fatigue loading in common usage include direct stress, where the material is repeatedly loaded in its axial direction; plane bending, where the material is bent about its neutral plane; rotating bending, where the specimen is being rotated and at the same time subjected to a bending moment; torsion, where the specimen is subjected to conditions which produce reversed or fluctuating torsional stresses and, finally, combined stress conditions, where two or more of the previous types of loading are operating simultaneously. It is therefore important that the method of stressing and type of machine used to carry out the fatigue test should always be quoted.

Within a fairly wide range of approximately 100 cycles/min to 6000 cycles/min, the effect of speed of testing (i.e. frequency of load cycling) on the fatigue strength of metals is small but, nevertheless, frequency may be important, particularly in polymers and other materials which show a large hysteresis loss. Test details should, therefore, always include the frequency of the stress cycle, this being chosen so as not to affect the result obtained (depending upon the material under test) the form of test piece and the type of machine used. Further details regarding fatigue testing procedure are given in BS3518: Parts 1 to 5.

Most fatigue tests are carried out at room temperature but often tests are also carried out at elevated or sub-zero temperatures depending upon the expected environmental operating conditions. At low temperatures the fatigue strength of metals show no deterioration and may even show a slight improvement, however, with increase in temperature, the fatigue strength decreases as creep effects are added to those of fatigue and this is revealed by a more pronounced effect of frequency of cycling and of mean stress since creep is both stress- and time-dependent.

When carrying out elevated temperature tests in air, oxidation of the sample may take place producing a condition similar to corrosion fatigue. Under the action of the cyclic stress, protective oxide films are cracked allowing further and more severe attack by the corrosive media. Thus fatigue and corrosion together ensure continuous propagation of cracks, and materials which show a definite fatigue limit at room temperature will not do so at elevated temperatures or at ambient temperatures under corrosive conditions – see Fig. 11.6.

11.1.2. P/S/N curves

The fatigue life of a component as determined at a particular stress level is a very variable quantity so that seemingly identical specimens may give widely differing results. This scatter

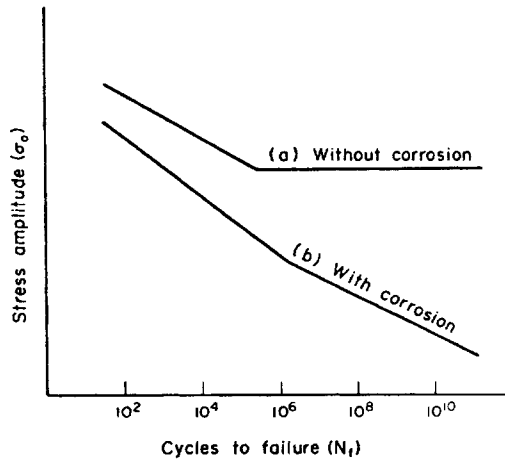


Fig. 11.6. The effect of corrosion on fatigue life. S/N Curve for (a) material showing fatigue limit; (b) same material under corrosion conditions.

arises from many sources including variations in material composition and heterogeneity, variations in surface finish, variations in axially of loading, etc.

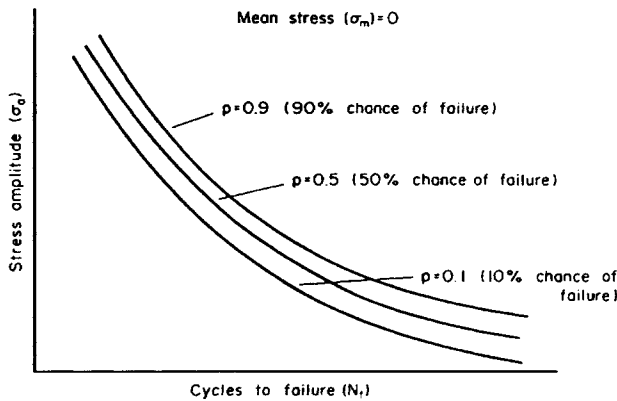


Fig. 11.7. P/S/N curves indicating percentage chance of failure for given stress level after known number of cycles (zero mean stress)

To overcome this problem, a number of test pieces should be tested at several different stresses and then an estimate of the life at a particular stress level for a given probability can be made. If the probability of 50% chance of failure is required then a P/S/N curve can be drawn through the median value of the fatigue life at the stress levels used in the test. It should be noted that this 50% ($p = 0.5$) probability curve is the curve often displayed in textbooks as *the* S/N curve for a particular material and if less probability of failure is required then the fatigue limit value will need to be reduced.

11.1.3. Effect of mean stress

If the fatigue test is carried out under conditions such that the mean stress is tensile (Fig. 11.3), then, in order that the specimen will fail in the same number of cycles as a similar specimen tested under zero mean stress conditions, the stress amplitude in the former case will have to be reduced. The fact that an increasing tensile mean stress lowers the fatigue or endurance limit is important, and all S/N curves should contain information regarding the test conditions (Fig. 11.8).

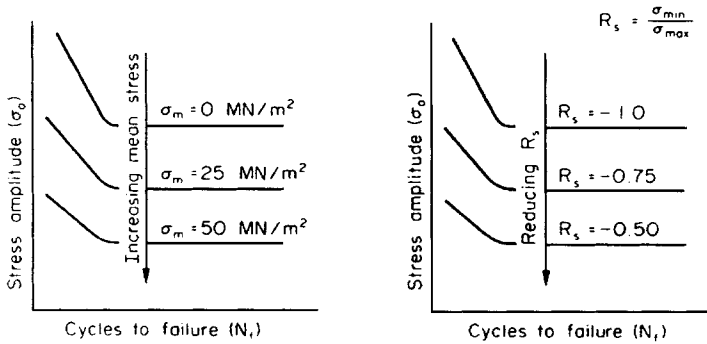


Fig. 11.8. Effect of mean stress on the S/N curve expressed in alternative ways.

A number of investigations have been made of the quantitative effect of *tensile mean stress* resulting in the following equations:

$$\text{Goodman}^{(1)} \quad \sigma_a = \sigma_N \left[1 - \left(\frac{\sigma_m}{\sigma_{TS}} \right) \right] \tag{11.7}$$

$$\text{Geber}^{(2)} \quad \sigma_a = \sigma_N \left[1 - \left(\frac{\sigma_m}{\sigma_{TS}} \right)^2 \right] \tag{11.8}$$

$$\text{Soderberg}^{(3)} \quad \sigma_a = \sigma_N \left[1 - \left(\frac{\sigma_m}{\sigma_y} \right) \right] \tag{11.9}$$

- where σ_N = the fatigue strength for N cycles under zero mean stress conditions.
- σ_a = the fatigue strength for N cycles under condition of mean stress σ_m .
- σ_{TS} = tensile strength of the material.
- σ_y = yield strength of the material.

The above equations may be shown in graphical form (Fig. 11.9) and in actual practice it has been found that most test results fall within the envelope formed by the parabolic curve of Geber and the straight line of Goodman. However, because the use of Soderberg gives an additional margin of safety, this is the equation often preferred – see Example 11.2.

Even when using the Soderberg equation it is usual to apply a factor of safety F to both the alternating and the steady component of stress, in which case eqn. (11.9) becomes:

$$\sigma_a = \frac{\sigma_N}{F} \left(1 - \frac{\sigma_m \times F}{\sigma_y} \right) \tag{11.10}$$

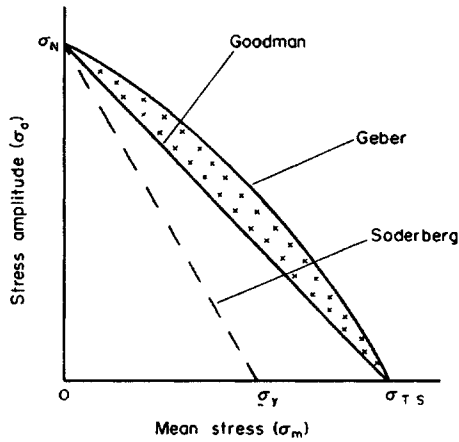


Fig. 11.9. Amplitude/mean stress relationships as per Goodman, Geber and Soderberg.

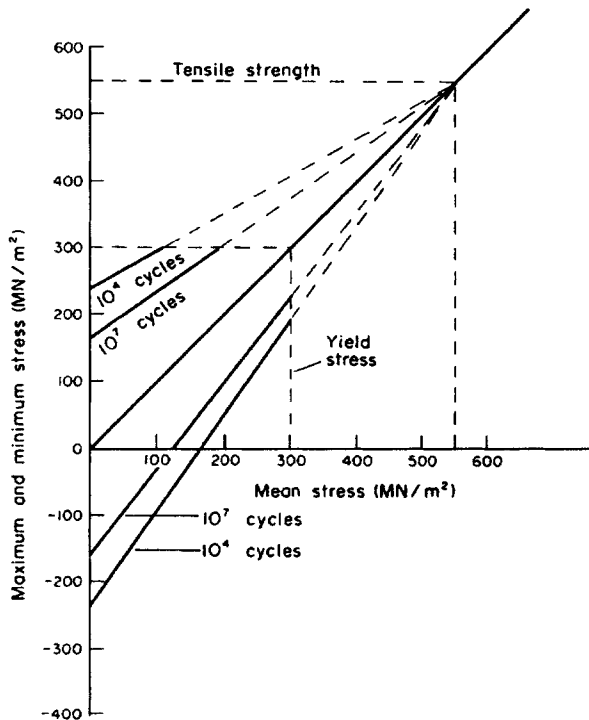


Fig. 11.10. Smith diagram.

The interrelationship of mean stress and alternating stress amplitude is often shown in diagrammatic form frequently collectively called Goodman diagrams. One example is shown in Fig. 11.10, and includes the experimentally derived curves for endurance limits of a specific steel. This is called a Smith diagram. Many alternative forms of presentation of data are possible including the Haigh diagram shown in Fig. 11.11, and when understood

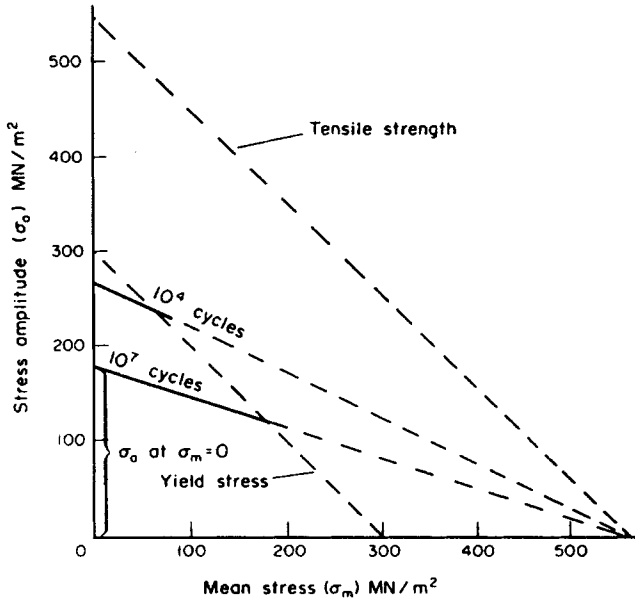


Fig. 11.11. Haigh diagram.

by the engineer these diagrams can be used to predict the fatigue life of a component under a particular stress regime. If the reader wishes to gain further information about the use of these diagrams it is recommended that other texts be consulted.

The effect of a *compressive mean stress* upon the life of a component is not so well documented or understood as that of a tensile mean stress but in general most materials do not become any worse and may even show an improved performance under a compressive mean stress. In calculations it is usual therefore to take the mean stress as zero under these conditions.

11.1.4. Effect of stress concentration

The influence of stress concentration (see §10.3) can be illustrated by consideration of an elliptical crack in a plate subjected to a tensile stress. Provided that the plate is very large, the “theoretical stress concentration” factor K_t is given by:

$$K_t = 1 + \frac{2A}{B} \quad (11.11)$$

where “A” and “B” are the crack dimensions as shown in Fig. 11.12.

If the crack is perpendicular to the direction of stress, then A is large compared with B and hence K_t will be large. If the crack is parallel to the direction of stress, then A is very small compared with B and hence $K_t = 1$. If the dimensions of A and B are equal such that the crack becomes a round hole, then $K_t = 3$ and a maximum stress of $3\sigma_{\text{nom}}$ acts at the sides of the hole.

The effect of sudden changes of section, notches or defects upon the fatigue performance of a component may be indicated by the “*fatigue notch*” or “*fatigue strength reduction*” factor

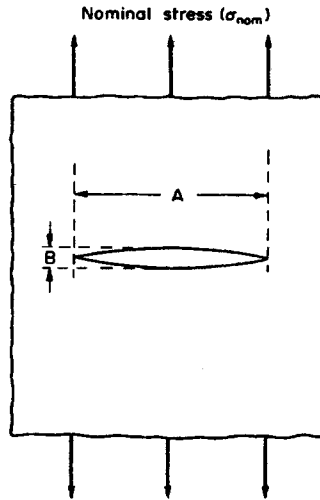


Fig. 11.12. Elliptical crack in semi-infinite plate.

K_f , which is the ratio of the stress amplitude at the fatigue limit of an un-notched specimen, to that of a notched specimen under the same loading conditions.

K_f is always less than the static theoretical stress concentration factor referred to above because under the compressive part of a tensile-compressive fatigue cycle, a fatigue crack is unlikely to grow. Also the ratio of K_f/K_t decreases as K_t increases, sharp notches having less effect upon fatigue life than would be expected. The extent to which the stress concentration effect under fatigue conditions approaches that for static conditions is given by the “notch sensitivity factor” q , and the relationship between them may be simply expressed by:

$$q = \frac{K_f - 1}{K_t - 1} \quad (11.12)$$

thus q is always less than 1. See also §10.3.5.

Notch sensitivity is a very complex factor depending not only upon the material but also upon the grain size, a finer grain size resulting in a higher value of q than a coarse grain size. It also increases with section size and tensile strength (thus under some circumstances it is possible to decrease the fatigue life by increasing tensile strength!) and, as has already been mentioned, it depends upon the severity of notch and type of loading.

In dealing with a ductile material it is usual to apply the factor K_f only to the fluctuating or alternating component of the applied stress. Equation (11.10) then becomes:

$$\sigma_a = \frac{\sigma_N}{F K_f} \left[1 - \left(\frac{\sigma_m F}{\sigma_y} \right) \right] \quad (11.13)$$

A typical application of this formula is given in Example 11.3.

11.1.5. Cumulative damage

In everyday, true-life situations, for example a car travelling over varying types of roads or an aeroplane passing through various weather conditions on its flight, stresses will not generally be constant but will vary according to prevailing conditions.

Several attempts have been made to predict the fatigue strength for such variable stresses using S/N curves for constant mean stress conditions. Some of the predictive methods available are very complex but the simplest and most well known is “*Miner’s Law*.”

Miner⁽⁷⁾ postulated that whilst a component was being fatigued, internal damage was taking place. The nature of the damage is difficult to specify but it may help to regard damage as the slow internal spreading of a crack, although this should not be taken too literally. He also stated that the extent of the damage was directly proportional to the number of cycles for a particular stress level, and quantified this by adding, “*The fraction of the total damage occurring under one series of cycles at a particular stress level, is given by the ratio of the number of cycles actually endured n to the number of cycles N required to break the component at the same stress level*”. The ratio n/N is called the “*cycle ratio*” and Miner proposed that failure takes place when the sum of the cycle ratios equals unity.

i.e. when

$$\Sigma n/N = 1$$

or

$$\frac{n_1}{N_1} + \frac{n_2}{N_2} + \frac{n_3}{N_3} + \dots + \text{etc} = 1 \quad (11.14)$$

If equation (11.14) is merely treated as an algebraic expression then it should be unimportant whether we put n_3/N_3 before n_1/N_1 etc., but experience has shown that the order of application of the stress is a matter of considerable importance and that the application of a higher stress amplitude first has a more damaging effect on fatigue performance than the application of an initial low stress amplitude. Thus the cycle ratios rarely add up to 1, the sum varying between 0.5 and 2.5, but it does approach unity if the number of cycles applied at any given period of time for a particular stress amplitude is kept relatively small and frequent changes of stress amplitude are carried out, i.e. one approaches random loading conditions. A simple application of Miner’s rule is given in Example 11.4.

11.1.6. Cyclic stress–strain

Whilst many components such as axle shafts, etc., have to withstand an almost infinite number of stress reversals in their lifetime, the stress amplitudes are relatively small and usually do not exceed the elastic limit. On the other hand, there are a growing number of structures such as aeroplane cabins and pressure vessels where the interval between stress cycles is large and where the stresses applied are very high such that plastic deformation may occur. Under these latter conditions, although the period in time may be long, the number of cycles to failure will be small and in recent years interest has been growing in this “*low cycle fatigue*”.

If, during fatigue testing under these high stress cycle conditions, stress and strain are continually monitored, a hysteresis loop develops characteristic of each cycle.

Figure 11.13 shows typical loops under constant stress amplitude conditions, each loop being displaced to the right for the sake of clarity. It will be observed that with each cycle, because of work hardening, the width of the loop is reduced, eventually the loop narrowing to a straight line under conditions of total elastic deformation.

The relationship between the loop width W and the number of cycles N is given by:

$$W = AN^{-h} \quad (11.15)$$

where A is a constant and h the measure of the rate of work hardening.

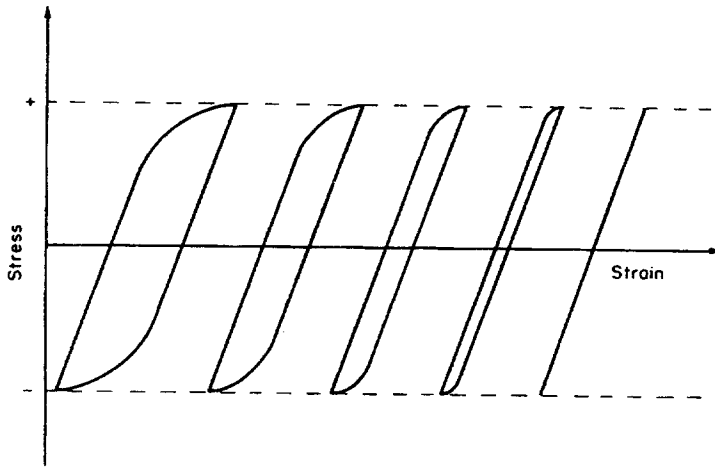


Fig. 11.13. Cyclic stress–strain under constant stress conditions – successive loading loops displaced to right for clarity. Hysteresis effects achieved under low cycle, high strain (constant stress amplitude) fatigue.

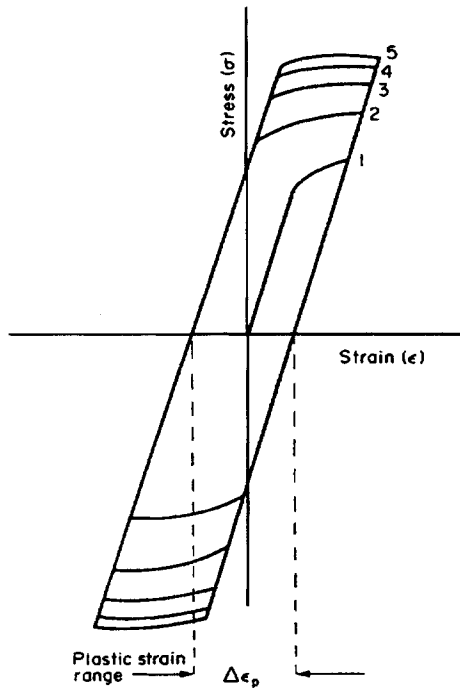


Fig. 11.14. Cyclic stress–strain under constant strain amplitude conditions.

If instead of using constant *stress* amplitude conditions, one uses constant *strain* amplitude conditions then the form of loop is indicated in Fig. 11.14. Under these conditions the stress range increases with the number of cycles but the extent of the increase reduces with each cycle such that after about 20% of the life of the component the loop becomes constant.

If now a graph is drawn (using logarithmic scales) of the plastic strain range against the number of cycles to failure a straight line results (Fig. 11.15). From this graph we obtain the following equation for the plastic strain range $\Delta\varepsilon_p$ which is known as the Coffin–Manson Law.⁽⁸⁾

$$\Delta\varepsilon_p = K(N_f)^{-b} \tag{11.16}$$

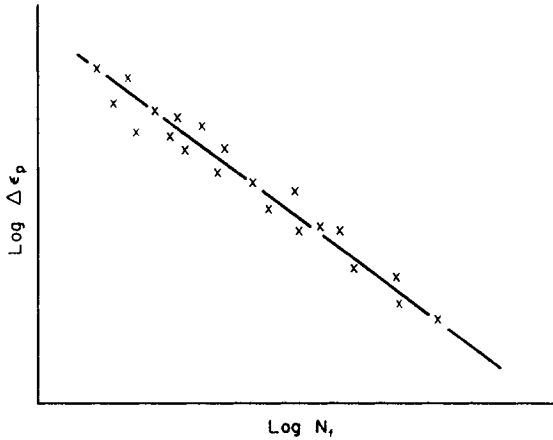


Fig. 11.15. Relationship between plastic strain and cycles to failure in low cycle fatigue.

The value of b varies between 0.5 and 0.6 for most metals, whilst the constant K can be related to the ductility of the metal. Equation (11.16) can also be expressed as:

$$\Delta\varepsilon_p = \left(\frac{N_f}{D}\right)^{-b} \tag{11.17}$$

where D is the ductility as determined by the reduction in area r in a tensile test.

i.e.
$$D = l_n \left(\frac{1}{1-r}\right)$$

In many applications, the total strain range may be known but it may be difficult to separate it into plastic and elastic components; thus a combined equation may be more useful.

$$\Delta\varepsilon_l = \Delta\varepsilon_e + \Delta\varepsilon_p$$

Where $\Delta\varepsilon_l$, $\Delta\varepsilon_e$ and $\Delta\varepsilon_p$ stand for total, elastic and plastic strain ranges respectively. Relationships between $\Delta\varepsilon_p$ and N_f are given above but $\Delta\varepsilon_e$ may be related to N_f by the following modified form of *Basquin's Law*.⁽⁹⁾

$$\Delta\varepsilon_e = 3.5 \times \frac{\sigma_{TS}}{E} \times N_f^{-0.12} \tag{11.18}$$

If a graph is plotted (Fig. 11.16) of strain range against number of cycles to failure, it can be seen that the beginning part of the curve closely fits the slope of Coffin's equation while the latter part fits the modified Basquin's equation, the cross-over point being at about 10^5

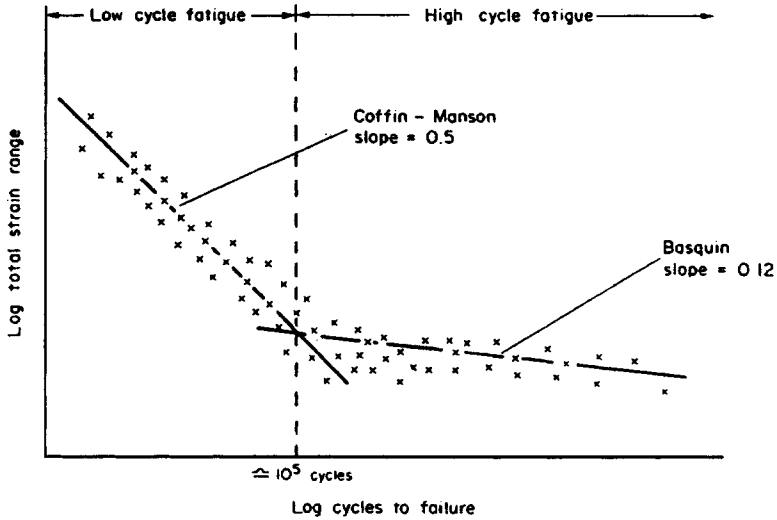


Fig. 11.16. Relationship between total strain and cycles to failure in low and high cycle fatigue.

cycles. Therefore, it can be said that up to this figure fatigue performance is a function of the material's ductility, whilst for cycles in excess of this, life is a function of the strength of the material.

11.1.7. Combating fatigue

When selecting a material for use under fatigue conditions it may be better to select one which shows a fatigue limit, e.g. steel, rather than one which exhibits an endurance limit, e.g. aluminium. This has the advantage of enabling the designer to design for an infinite life provided that the working stresses are kept to a suitably low level, whereas if the latter material is selected then design must be based upon a finite life.

In general, for most steels, the fatigue limit is about 0.5 of the tensile strength, therefore, by selecting a high-strength material the allowable working stresses may be increased. Figure 11.17.

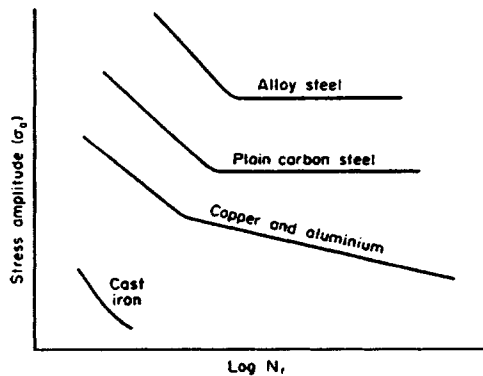


Fig. 11.17. Relative performance of various materials under fatigue conditions.

Following on the above, any process that increases tensile strength should raise the fatigue limit and one possible method of accomplishing this with steels is to carry out heat treatment. The general effect of heat treatment on a particular steel is shown in Fig. 11.18.

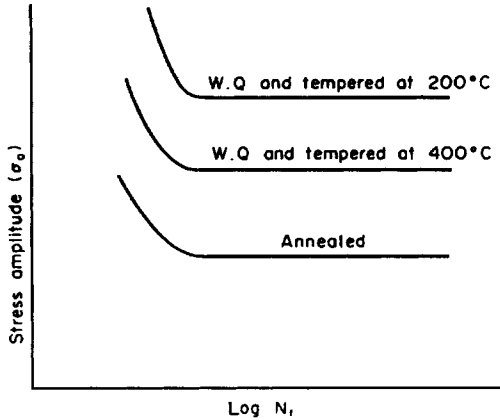


Fig. 11.18. Effect of heat treatment upon the fatigue limit of steel.

Sharp changes in cross-section will severely reduce the fatigue limit (see §10.3.4), and therefore generous radii can be used to advantage in design. Likewise, surface finish will also have a marked effect and it must be borne in mind that fatigue data obtained in laboratory tests are often based upon highly polished, notch-free, samples whilst in practice the component is likely to have a machined surface and many section changes. The sensitivity of a material to notches tends to increase with increase in tensile strength and decrease with increase in plasticity, thus, in design situations, a compromise between these opposing factors must be reached.

Figure 11.19 shows the fatigue limits of typical steels in service expressed as a percentage of the fatigue limits obtained for the same steels in the laboratory and it will be noticed that

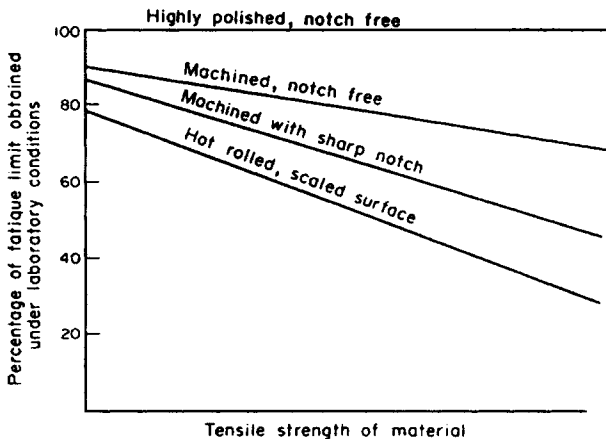


Fig. 11.19. Effect of surface conditions on the fatigue strength of materials.

the fatigue limit of a low-strength steel is not affected to the same extent as the high-strength steel. i.e. the former is less notch-sensitive (another factor to be taken account of when looking at the relative cost of the basic material). However, it must be pointed out that it may be poor economy to overspecify surface finish, particularly where stress levels are relatively low.

Because fatigue cracks generally initiate at the surface of a component under tensile stress conditions, certain processes, both chemical and mechanical, which introduce residual surface compressive stresses may be utilised to improve fatigue properties (see §10.2). However, the extent of the improvement is difficult to assess quantitatively at this juncture of time. Among the chemical treatments, the two most commonly employed are *carburising* and *nitriding* which bring about an expansion of the lattice at the metal surface by the introduction of carbon and nitrogen atoms respectively. Figure 11.20 shows the effect upon fatigue limit.

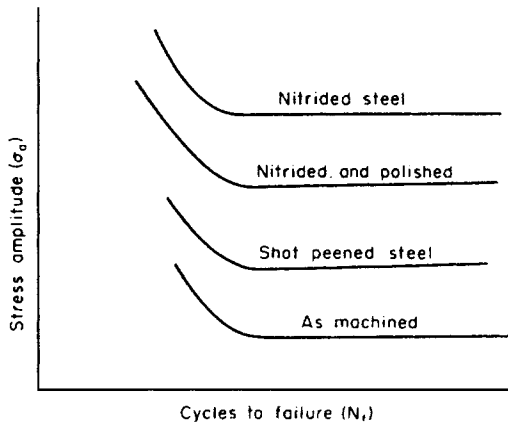


Fig. 11.20. Effect of processes which introduce surface residual stresses upon the fatigue strength of a steel.

The most popular mechanical method of improving fatigue limits is *shot peening*, the surface of the material being subjected to bombardment by small pellets or shot of suitable material. In this manner, compressive residual stresses are induced but only to a limited depth, roughly 0.25 mm. Other mechanical methods involve improving fatigue properties around holes by pushing through balls which are slightly over-sized – a process called “*ballising*,” and the use of balls or a roller to cold work shoulders on fillets – a process called “*rolling*”.

11.1.8. Slip bands and fatigue

The onset of fatigue is usually characterised by the appearance on the surface of the specimen of slip bands which, after about 5% of the fatigue life, become permanent and cannot be removed by electropolishing. With increase in the number of load cycles these bands deepen until eventually a crack is formed.

Using electron microscopical techniques Forsyth⁽¹⁰⁾ observed *extrusions* and *intrusions* from well-defined slip bands and Cottrell⁽¹¹⁾ proposed a theory of cross-slip or slip on alternate slip planes whereby, during the tensile half of the stress cycle, slip occurs on each plane in turn to produce two surface steps which on the compressive half of the cycle are

converted into an intrusion and an extrusion (see Fig. 11.21). Although an intrusion is only very small, being approximately $1\ \mu\text{m}$ deep, it nevertheless can act as a stress raiser and initiate the formation of a true fatigue crack.

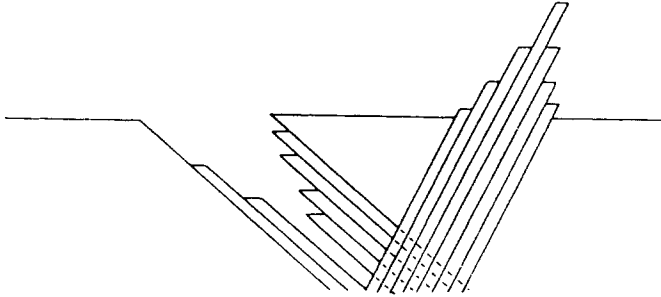


Fig. 11.21. Diagrammatic representation of the formation of intrusions and extrusions.

Fatigue endurance is commonly divided into two periods: (i) the “*crack initiation*” period; (ii) the “*crack growth*” or “*propagation*” period. It is now accepted that the fatigue crack is initiated by the deepening of the slip band grooves by dislocation movement into crevices and finally cracks, but this makes it very difficult to distinguish between crack initiation and crack propagation and therefore a division of the fatigue based upon mode of crack growth is often more convenient.

Initially the cracks will form in the surface grains and develop along the active slip plane as mentioned briefly above. These cracks are likely to be aligned with the direction of maximum shear within the component, i.e. at 45° to the maximum tensile stress. This is often referred to as *Stage I growth* and is favoured by zero mean stress and low cyclic stress conditions.

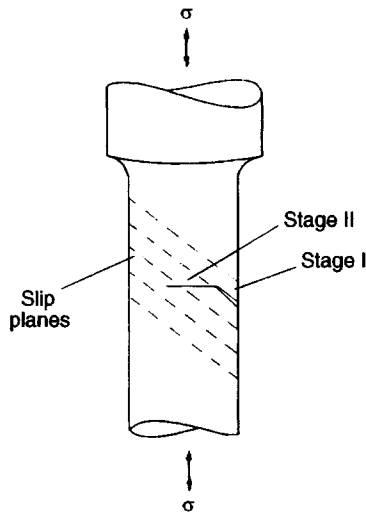


Fig. 11.22. Stage I and II fatigue crack propagation.

At some point, usually when the crack encounters a grain boundary. Stage I is replaced by *Stage II growth* in which the crack is normal to the maximum principal tensile stress. This stage is favoured by a tensile mean stress and high cyclic stress conditions. Close examination of the fractured surface shows that over that part associated with Stage II, there are a large number of fine lines called "*striations*", each line being produced by one fatigue cycle and by measuring the distance between a certain number of striations the fatigue crack growth rate can be calculated.

Once the fatigue crack has reached some critical length such that the energy for further growth can be obtained from the elastic energy of the surrounding metal, catastrophic failure takes place. This final fracture area is rougher than the fatigue growth area and in mild steel is frequently crystalline in appearance. Sometimes it may show evidence of plastic deformation before final separation occurred. Further discussion of fatigue crack growth is introduced in §11.3.7.

11.2. Creep

Introduction

Creep is the time-dependent deformation which accompanies the application of stress to a material. At room temperatures, apart from the low-melting-point metals such as lead, most metallic materials show only very small creep rates which can be ignored. With increase in temperature, however, the creep rate also increases and above approximately $0.4 T_m$, where T_m is the melting point on the Kelvin scale, creep becomes very significant. In high-temperature engineering situations related to gas turbine engines, furnaces and steam turbines, etc., deformation caused by creep can be very significant and must be taken into account.

11.2.1. The creep test

The creep test is usually carried out at a constant temperature and under constant load conditions rather than at constant stress conditions. This is acceptable because it is more representative of service conditions. A typical creep testing machine is shown in Fig. 11.23. Each end of the specimen is screwed into the specimen holder which is made of a creep-resisting alloy and thermocouples and accurate extensometers are fixed to the specimen in order to measure temperature and strain. The electric furnace is then lowered into place and when all is ready and the specimen is at the desired temperature, the load is applied by adding weights to the lower arm and readings are taken at periodic intervals of extension against time. It is important that accurate control of temperature is possible and to facilitate this the equipment is often housed in a temperature-controlled room.

The results from the creep test are plotted in graphical form to produce a typical curve as shown in Fig. 11.24. After the initial extension OA which is produced as soon as the test load is applied, and which is not part of the creep process proper (but which nevertheless should not be ignored), the curve can be divided into three stages. In the first or *primary* stage AB , the movement of dislocations is very rapid, any barriers to movement caused by work-hardening being overcome by the recovery processes, albeit at a decreasing rate. Thus the initial *creep strain rate* is high but it rapidly decreases to a constant value. In the

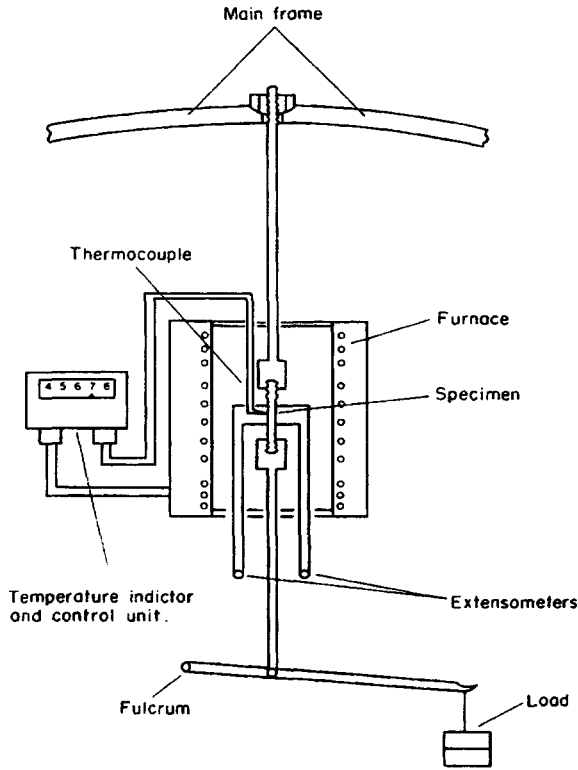


Fig. 11.23. Schematic diagram of a typical creep testing machine.

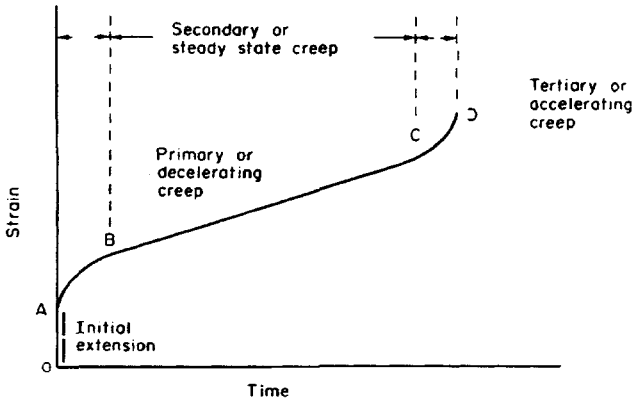


Fig. 11.24. Typical creep curve.

secondary stage *BC*, the work-hardening process of “dislocation pile-up” and “entanglement” are balanced by the recovery processes of “dislocation climb” and “cross-slip”, to give a straight-line relationship and the slope of the graph in this steady-state portion of the curve is equal to the secondary creep rate. Since, generally, the primary and tertiary stages occur quickly, it is the secondary creep rate which is of prime importance to the design engineer.

The third or *tertiary* stage *CD* coincides with the formation of internal voids within the specimen and this leads to “necking”, causing the stress to increase and rapid failure to result.

The shape of the creep curve for any material will depend upon the temperature of the test and the stress at any time since these are the main factors controlling the work-hardening and recovery processes. With increase in temperature, the creep rate increases because the softening processes such as “dislocation climb” can take place more easily, being diffusion-controlled and hence a thermally activated process.

It is expected, therefore, that the creep rate is closely related to the *Arrhenius equation*, viz.:

$$\epsilon_s^0 = A e^{-H/RT} \quad (11.19)$$

where ϵ_s^0 is the *secondary creep rate*, H is the *activation energy* for creep for the material under test, R is the universal gas constant, T is the absolute temperature and A is a constant. It should be noted that both A and H are not true constants, their values depending upon stress, temperature range and metallurgical variables.

The secondary creep rate also increases with increasing stress, the relationship being most commonly expressed by the *power law equation*:

$$\epsilon_s^0 = \beta \sigma^n \quad (11.20)$$

where β and n are constants, the value of n usually varying between 3 and 8.

Equations (11.19) and (11.20) may be combined to give:

$$\epsilon_s^0 = K \sigma^n e^{-H/RT} \quad (11.21)$$

Figure 11.25 illustrates the effect of increasing stress or temperature upon the creep curve and it can be seen that increasing either of these two variables results in a similar change of creep behaviour, that is, an increase in the secondary or minimum creep rate, a shortening of the secondary creep stage, and the earlier onset of tertiary creep and fracture.

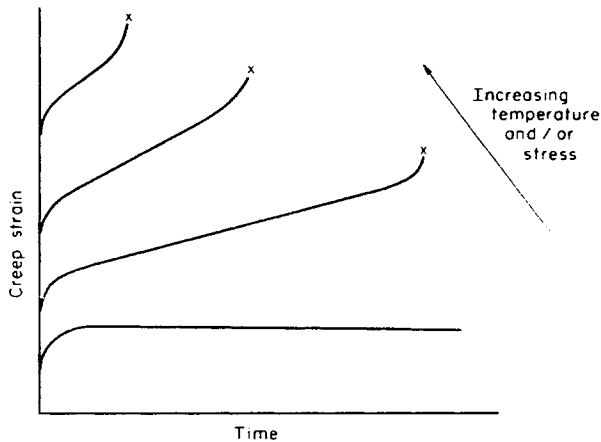


Fig. 11.25. Creep curves showing effect of increasing temperature or stress.

11.2.2. Presentation of creep data

When dealing with problems in which creep is important, the design engineer may wish to know whether the creep strain over the period of expected life of the component is tolerable, or he may wish to know the value of the maximum operating stress if the creep strain is not to exceed a specified figure over a given period of time.

In order to assist in the answering of these questions, creep data are often published in other forms than the standard strain-time curve. Figure 11.26 shows a number of fixed strain curves presented in the form of an *isometric stress-time* diagram which relates strain, stress and time for a fixed, specified, temperature and material, while Fig. 11.27 is an *isometric strain-time* diagram.

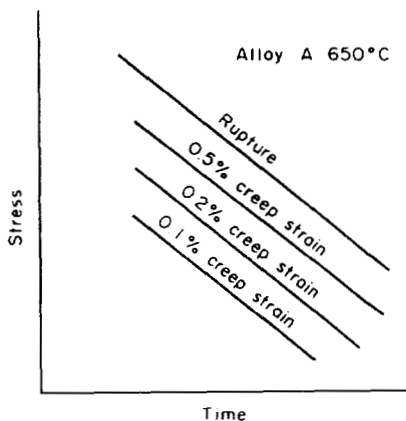


Fig. 11.26. Isometric stress-time diagrams.

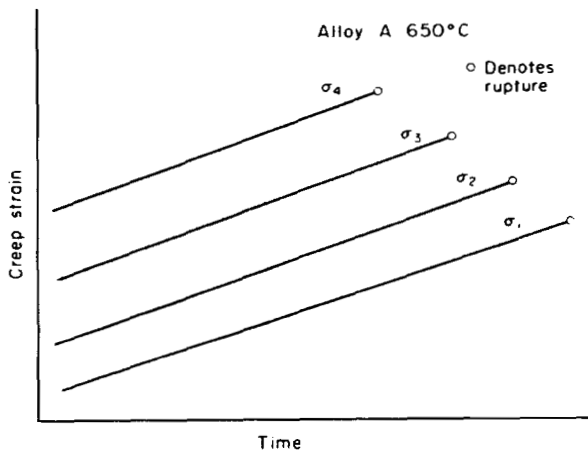


Fig. 11.27. Isometric strain-time diagram.

Sometimes, instead of presenting data relating to a fixed temperature, the strain may be constant and curves of equal time called *isochronous stress–temperature curves*. Fig. 11.28 may be given. Such curves can be used for comparing the properties of various alloys and Fig. 11.29 shows relations for a creep strain of 0.2% in 3000 hours. Such information might be applicable to an industrial gas turbine used intermittently.

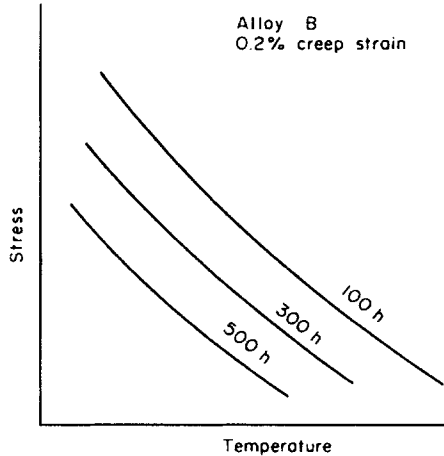


Fig. 11.28. Isochronous stress–temperature curves.

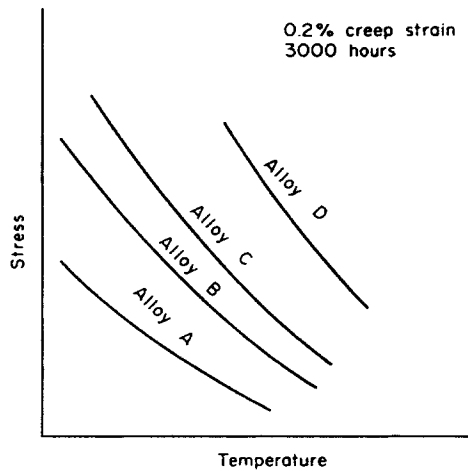


Fig. 11.29. 3000 hours, 0.2% creep–strain curves for various alloys.

11.2.3. The stress–rupture test

Where creep strain is the important design factor and fracture may be expected to take a very long time, the test is often terminated during the steady state of creep when sufficient

information has been obtained to produce a sufficiently accurate value of the secondary creep rate. Where life is the important design parameter, then the test is carried out to destruction and this is known as a *stress-rupture test*.

Because the total strain in a rupture test is much higher than in a creep test, the equipment can be less sophisticated. The loads used are generally higher, and thus the time of test shorter, than for creep. The percentage elongation and percentage reduction in area at fracture may be determined but the principal information obtained is the time to failure at a fixed temperature under nominal stress conditions.

A graph (Fig. 11.30), is plotted of time to rupture against stress on a log-log basis, and often a straight line results for each test temperature. Any change in slope of this stress-rupture line may be due to change in the mechanism of creep rupture within the material.

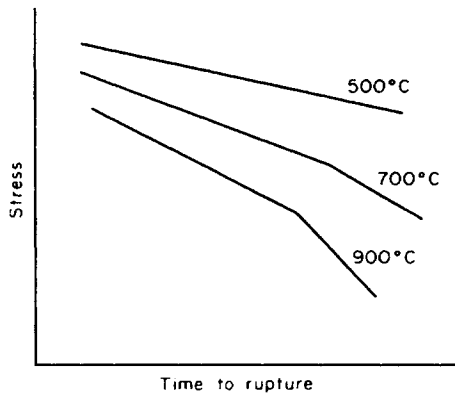


Fig. 11.30. Stress-rupture time curves at various temperatures.

11.2.4. Parameter methods

Very often, engineers have to confirm to customers that a particular component will withstand usage at elevated temperatures for a particular life-time which, in the case of furnace equipment or steam applications, may be a considerable number of years. It is impracticable to test such a component, for example, for twenty years before supplying the customer and therefore some method of extrapolation is required. The simplest method is to test at the temperature of proposed usage, calculate the minimum creep rate and assume that this will continue for the desired life-time and then ascertain whether the creep strain is acceptable. The obvious disadvantage of this method is that it does not allow for tertiary creep and sudden failure (which the creep curve shows will take place at some time in the future but at a point which cannot be determined because of time limitations).

In order to overcome this difficulty a number of workers have proposed methods involving accelerated creep tests, whereby the test is carried out at a higher temperature than that used in practice and the results used to predict creep-life or creep-strain over a longer period of time at a lower temperature.

The most well-known method is that of *Larson and Miller* and is based upon the Arrhenius equation (eqn. 11.19) which can be rewritten, in terms of \log_{10} as in eqn. (11.22) or in terms

of l_n without the constant 0.4343.

$$\log_{10} t_r = \log_{10} G + 0.4343 \cdot \frac{H}{R} \cdot \frac{1}{T} \quad (11.22)$$

where t_r is the time to rupture, G is a constant, T is the **absolute temperature**, R is the universal gas constant, and H is the activation energy for creep and is assumed to be stress-dependent.

$$\therefore \log_{10} t_r + C = m \cdot \frac{1}{T}$$

where m is a function of stress.

$$\therefore T(\log_{10} t_r + C) = m$$

this can be re-written as:

$$P_1 = f(\sigma)$$

where the *Larson–Miller parameter*

$$P_1 = T(\log_{10} t_r + C) \quad (11.23)$$

the value of the constant C can be obtained from the intercept when $\log_{10} t_r$ is plotted against $1/T$. For ferrous metals it usually lies between 15 and 30. If a test is carried out under a certain value of stress and temperature, the value of t_r can be determined and, if repeated for other stress and temperature values, the results can be plotted on a *master curve* (Fig. 11.31).

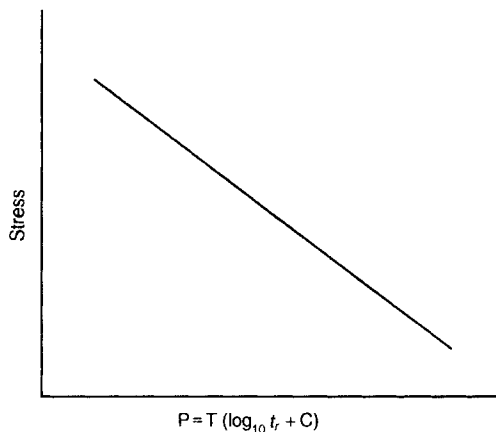


Fig. 11.31. Larson–Miller master curve.

The value of the parameter P is the same for a wide variety of combinations of t_r and temperature, ranging from short times and high temperatures representing test conditions, to long times at lower temperatures representing service conditions.

Results obtained by other workers, notably Sherby and Dorn⁽¹⁴⁾, suggest that G in the above equation (eqn. 11.22) is not a true constant but varies with stress whilst E is essentially constant. If $0.4343 E/R$ in eqn. (11.22) is replaced by α and $\log_{10} G$ by ϕ then eqn. (11.22)

can be written as:

$$\log_{10} t_r - \frac{\alpha}{T} = \phi$$

or

$$P_2 = f(\sigma)$$

where the *Sherby–Dorn parameter*

$$P_2 = \log_{10} t_r - \frac{\alpha}{T} \tag{11.24}$$

the constant α being determined from the common slope of a plot of $\log_{10} t_r$ versus $1/T$. After a series of creep tests, a master curve can then be plotted and used in the same manner as for the Larson–Miller parameter.

Another parameter was suggested by Manson and Haferd⁽¹³⁾ who found that, for a given material under different stress and temperature conditions, a family of lines was obtained which intercepted at a point when $\log t_r$ was plotted against T . The family of lines of this kind could be represented by the equation:

$$T - T_a = m(\log_{10} t_r - \log_{10} t_a) \tag{11.25}$$

where the slope m is a function of stress and T_a and $\log_{10} t_a$ are the coordinates of the converging point (Fig. 11.32).

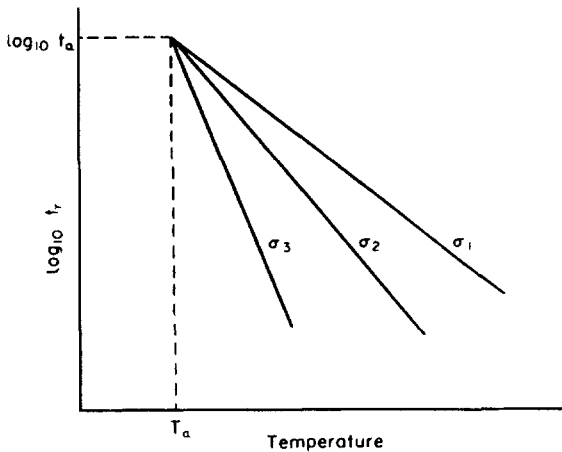


Fig. 11.32. Manson and Haferd curves.

The *Manson–Haferd parameter* can then be stated as:

$$P_3 = \frac{T - T_a}{\log_{10} t_r - \log_{10} t_a} \tag{11.26}$$

where $P_3 = m = f(\sigma)$.

A master curve can then be plotted in a similar manner to the other methods.

When using any of the above methods, certain facts should be borne in mind with regard to their limitations. Firstly, since the different methods give slightly differing results, this casts

doubts on the validity of all three methods and, in general, although the Manson–Haferd parameter has been found to produce more accurate predictions, it is difficult to determine the exact location of the point of convergence of the lines. Secondly, if one is using higher test temperatures than operating temperatures then the mechanisms of creep may be different and unrelated one to the other. Thirdly, the mechanism of creep failure may change with temperature; at lower temperatures, failure is usually transcrystalline whilst at higher temperatures it is intercrystalline, the change-over point being the *equi-cohesive temperature*. Results above this temperature are difficult to correlate with those obtained below this temperature.

11.2.5. Stress relaxation

So far we have been concerned with the study of material behaviour under constant loading or *constant stress* conditions where increase in strain is taking place and may eventually lead to failure. However, there are important engineering situations involving cylinder-head bolts, rivets in pressure vessels operating at elevated temperatures, etc., where we consider the *strain* to be *constant* and then we need to evaluate the decrease in stress which may take place. This time-dependent decrease in stress under constant strain conditions is called “*stress relaxation*”.

Consider two plates held together by a bolt deformed by a stress σ_i producing an initial strain ε_i which is all elastic.

$$\text{Then} \quad \varepsilon_i = \varepsilon_e = \sigma_i/E \quad (1)$$

At elevated temperatures and under conditions of steady-state creep, this bolt will tend to elongate at a rate ε^0 dictated by the power law:

$$\varepsilon^0 = \frac{d\varepsilon_c}{dt} = \beta\sigma^n \quad (2)$$

and, assuming the thickness of the plates remain constant, the strain caused by creep ε_c simply reduces the elastic part ε_e of the initial strain,

$$\text{i.e.} \quad \varepsilon_e = \varepsilon_i - \varepsilon_c \quad (3)$$

But, since the creep strain decreases the elastic component of the initial strain, a corresponding decrease in stress must also result from eqn. (1).

Since ε_i is constant, if we differentiate eqn. (3) with respect to time we obtain:

$$\frac{d\varepsilon_e}{dt} = -\frac{d\varepsilon_c}{dt} \quad (4)$$

but $\varepsilon_e = \sigma/E$ where σ is the instantaneous stress, therefore the LHS of eqn. (4) can be replaced by $(1/E) \cdot (d\sigma/dt)$ whilst, from eqn. (2), the RHS of eqn. (4) can be replaced by $\beta\sigma^n$.

Therefore, eqn. (4) can be rewritten:

$$\frac{1}{E} \cdot \frac{d\sigma}{dt} = -\beta\sigma^n \quad (5)$$

$$\therefore \int \frac{d\sigma}{\sigma^n} = -E\beta \int dt$$

$$\therefore -\frac{1}{(n-1)\sigma^{n-1}} = -E\beta t + C \quad (6)$$

To find C , consider the time $t = 0$, when the stress would be the initial stress σ_i

$$\text{Then } C = -\frac{1}{(n-1)\sigma_i^{n-1}} \quad (7)$$

substituting for C in eqn. (6), multiplying through by $(n-1)$ and re-arranging, gives:

$$\frac{1}{\sigma^{n-1}} = \frac{1}{\sigma_i^{n-1}} + \beta E(n-1)t \quad (11.27)$$

11.2.6. Creep-resistant alloys

The time-dependent deformation called “creep”, as with all deformation processes, is largely dependent upon dislocation movement and, therefore, the development of alloys with a high resistance to creep involves producing a material in which movement of dislocations only takes place with difficulty.

Since creep only becomes an engineering problem above about $0.4 \times$ melting point temperature on the Kelvin scale T_m , the higher the melting point of the major alloy constituent the better. However, there are practical limitations; for instance, some high-melting-point metals e.g. tungsten (M.Pt 3377°C) are difficult to machine, some Molybdenum (M.Pt 2607°C) form volatile oxides and some others, e.g. Osmium (M.Pt 3027°C) are very expensive and therefore Nickel (M.Pt 1453°C) and Cobalt (M.Pt 1492°C) are used extensively at the moment.

The movement of dislocations will be hindered to a greater extent in an alloy rather than in a pure metal and alloying elements such as chromium and cobalt are added therefore to produce a solid-solution causing “*solid-solution-hardening*”. Best results are obtained by rising an alloying element whose atomic size and valency are largely different from those of the parent metal, but this limits the amount that may be added. Also, the greater the amount of alloying element, the lower is likely to be the melting range of the alloy. Thus, the benefits of solution-hardening which hinders the dislocation movement may be outweighed at higher temperatures by a close approach to the solidus temperature.

Apart from solution-hardening, most creep-resisting alloys are further strengthened by *precipitation hardening* which uses carbides, oxides, nickel-titanium-aluminium, and nitride particles to block dislocation movement. Further deformation can then only take place by the dislocation rising above or “climbing” over the precipitate in its path and this is a diffusion-controlled process. Thus, metals with a low rate of self-diffusion e.g. face-centered-metals such as nickel are preferred to body-centred-metals.

Finally, *cold-working* is another method of increasing the high-temperature strength of an alloy and hindering dislocation movement but, since cold work lowers the re-crystallization temperature, for best results it is limited to about 15–20%. The use of alloying elements which raise the re-crystallization temperature in these circumstances will be beneficial.

All the methods above have their limitations. In solid-solution-hardening, a temperature increase will produce a corresponding increase in the mobility of the solute atoms which tend to lock the dislocations, thus making dislocation movement easier. With precipitation hardening, the increase in temperature may produce “*over-ageing*”, resulting in a coarsening of the precipitate or even a complete solution of the precipitate, both effects resulting in

a softening and decrease in creep resistance. It may be possible, however, to arrange for a second precipitate to form which may strengthen the alloy. The effects of cold work are completely nullified when the temperature rises above the re-crystallisation temperature, hence the application of this technique is very limited.

At room temperature, grain boundaries are normally stronger than the grain material but, with increase in temperature, the strength of the boundary decreases at a faster rate than does the strength of the grain interior such that above the “*equi-cohesive temperature*” (Fig. 11.33), a coarse-grain material will have higher strength than a fine-grain material since the latter is associated with an increase in the amount of grain boundary region. It should be noted that T_e is not fixed, but dependent upon stress, being higher at high stresses than at low stresses.

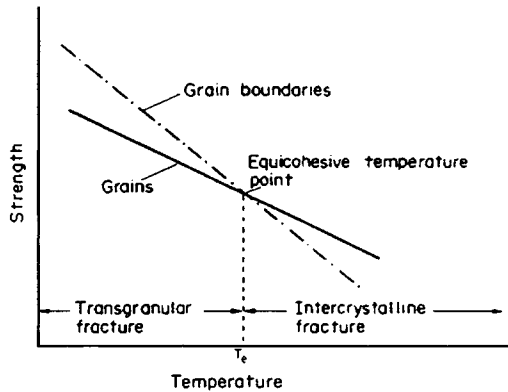


Fig. 11.33. Diagram showing concept of equi-cohesive temperature (T_e)

It can be shown also that creep rate is inversely proportional to the square of the grain size and dictated by the following formula:

$$\text{Creep rate} = \frac{K \sigma D}{d^2 T} \quad (11.28)$$

where K is a constant, σ is the applied stress, D is the coefficient of self diffusion, d is the grain size and T is the temperature. Thus, *grain boundary strengthening*, by the introduction of grain boundary carbide precipitates which help to prevent grain boundary sliding, and the control of grain size are important. Better still, the component may be produced from a single crystal such as the RB211 intermediate pressure turbine blade.

Apart from high creep resistance, alloys for use at high temperatures generally require other properties such as high oxidation resistance, toughness, high thermal fatigue resistance and low density, the importance of these factors depending upon the application of the material, and it is doubtful if any single test would provide a simple or accurate index of the qualities most desired.

11.3. Fracture mechanics

Introduction

The use of stress analysis in modern design procedures ensures that in normal service very few engineering components fail because they are overloaded. However, weakening of the

component by such mechanisms as corrosion or fatigue-cracking may produce a catastrophic fracture and in some instances, such as in the design of motorcycle crash helmets, the fracture properties of the component are the most important consideration. The study of how materials fracture is known as *fracture mechanics* and the resistance of a material to fracture is colloquially known as its “*toughness*”.

No structure is entirely free of defects and even on a microscopic scale these defects act as stress-raisers which initiate the growth of cracks. The theory of fracture mechanics therefore assumes the pre-existence of cracks and develops criteria for the catastrophic growth of these cracks. The designer must then ensure that no such criteria can be met in the structure.

In a stressed body, a crack can propagate in a combination of the three opening modes shown in Fig. 11.34. *Mode I* represents opening in a purely tensile field while *modes II* and *III* are in-plane and anti-plane shear modes respectively. The most commonly found failures are due to cracks propagating predominantly in mode I, and for this reason materials are generally characterised by their resistance to fracture in that mode. The theories examined in the following sections will therefore consider mode I only but many of the conclusions will also apply to modes II and III.

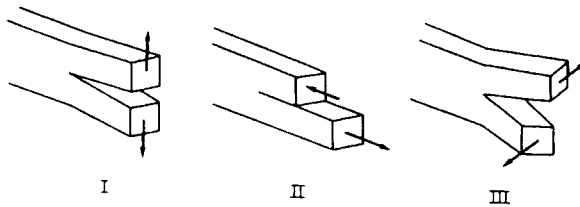


Fig. 11.34. The three opening modes, associated with crack growth: mode I–tensile; mode II–in-plane shear; mode III–anti-plane shear.

11.3.1. Energy variation in cracked bodies

A basic premise in thermodynamic theory is that a system will move to a state where the free energy of the system is lower. From this premise a simple criterion for crack growth can be formulated. It is assumed that a crack will only grow if there is a decrease in the free energy of the system which comprises the cracked body and the loading mechanism. The first usable criterion for fracture was developed from this assumption by Griffith⁽¹⁵⁾, whose theory is described in detail in §11.3.2.

For a clearer understanding of Griffith’s theory it is necessary to examine the changes in stored elastic energy as a crack grows. Consider, therefore, the simple case of a strip containing an edge crack of length *a* under uniaxial tension as shown in Fig. 11.35. If load *W* is applied gradually, the load points will move a distance *x* and the strain energy, *U*, stored in the body will be given by

$$U = \frac{1}{2}Wx$$

for purely elastic deformation.

The load and displacement are related by the “*compliance*” *C*,

i.e. (11.29)

$$x = CW$$

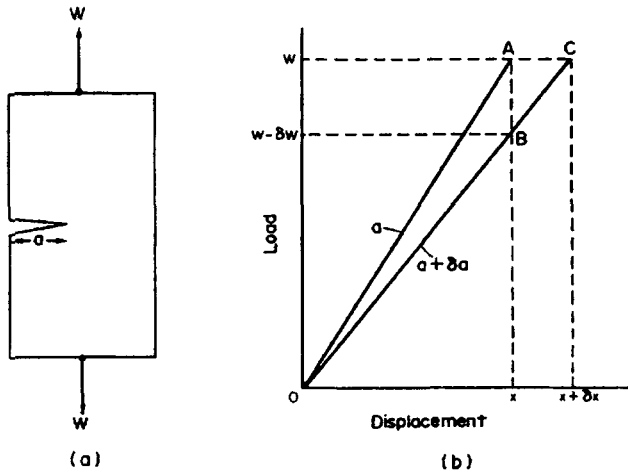


Fig. 11.35. (a) Cracked body under tensile load W ; (b) force-displacement curves for a body with crack lengths a and $a + da$.

The compliance is itself a function of the crack length but the exact relationship varies with the geometry of the cracked body. However, if the crack length increases, the body will become less stiff and the compliance will increase.

There are two limiting conditions to be considered depending on whether the cracked body is maintained at (a) constant displacement or (b) constant loading. Generally a crack will grow with both changing loads and displacement but these two conditions represent the extreme constraints.

(a) Constant displacement

Consider the case shown in Fig. 11.35(b). If the body is taken to be perfectly elastic then the load–displacement relationship will be linear. With an initial crack length a loading will take place along the line OA . If the crack extends a small distance δa while the points of application of the load remain fixed, there will be a small increase in the compliance resulting in a decrease in the load of δW . The load and displacement are then given by the point B . The change in stored energy will then be given by

$$\begin{aligned}\delta U_x &= \frac{1}{2}(W - \delta W)x - \frac{1}{2}Wx \\ \delta U_x &= -\frac{1}{2}\delta Wx\end{aligned}\quad (11.30)$$

(b) Constant loading

In this case, if the crack again extends a small distance δa the loading points must move through an additional displacement δx in order to keep the load constant. The load and displacement are then represented by the point C .

There would appear to be an increase in stored energy given by

$$\begin{aligned}\delta U &= \frac{1}{2}W(x + \delta x) - \frac{1}{2}Wx \\ &= \frac{1}{2}W\delta x\end{aligned}$$

However, the load has supplied an amount of energy

$$= W \delta x$$

This has to be obtained from external sources so that there is a total reduction in the potential energy of the system of

$$\begin{aligned} \delta U_w &= \frac{1}{2} W \delta x - W \delta x \\ \delta U_w &= -\frac{1}{2} W \delta x \end{aligned} \quad (11.31)$$

For infinitesimally small increases in crack length the compliance C remains essentially constant so that

$$\delta x = C \delta W$$

Substituting in eqn. (11.31)

$$\delta U_w = -\frac{1}{2} W C \delta W = -\frac{1}{2} x \delta W$$

Comparison with eqn. (11.30) shows that, for small increases in crack length,

$$\delta U_w = \delta U_x$$

It is therefore evident that for small increases in crack length there is a similar decrease in potential energy no matter what the loading conditions. For large changes in crack length there is no equality but, generally, we are interested in the onset of crack growth since for monotonic (continuously increasing) loading catastrophic failure commonly follows crack initiation.

If there is a decrease in potential energy when a crack grows then there must be an energy requirement for the production of a crack – otherwise all cracked bodies would fracture instantaneously. The following section examines the most commonly used fracture criterion based on a net decrease in energy.

11.3.2. Linear elastic fracture mechanics (L.E.F.M.)

(a) Griffith's criterion for fracture

Griffith's thermodynamics approach was the first to produce a usable theory of fracture mechanics.⁽¹²⁾ His theoretical model shown in Fig. 11.36 was of an infinite sheet under a remotely applied uniaxial stress σ and containing a central crack of length $2a$. The preceding section has shown that when a crack grows there is a decrease in potential energy. Griffith, by a more mathematically rigorous treatment, was able to show that if that decrease in energy is greater than the energy required to produce new crack faces then there will be a net decrease in energy and the crack will propagate. For an increase in crack length of δa .

$$\delta U = 2\gamma b \delta a$$

γ is the surface energy of the crack faces;

b is the thickness of the sheet.

At the onset of crack growth, δa is small and we have

$$\frac{dU}{da} = 2b\gamma$$

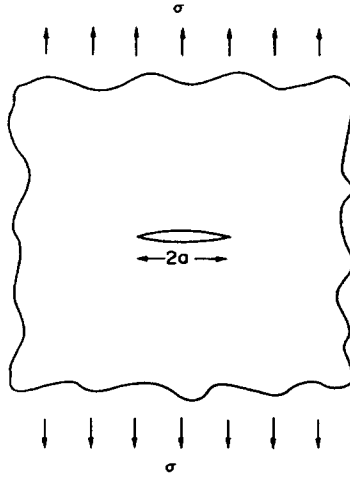


Fig. 11.36. Mathematical model for Griffith's analysis.

The expression on the left-hand side of the above equation is termed the “critical strain energy release” (with respect to crack length) and is usually denoted as G_c , i.e., at the onset of fracture,

$$G_c = \frac{\partial U}{\partial a} = 2b\gamma \quad (11.32)$$

This is the *Griffith criterion for fracture*.

Griffith's analysis gives G_c in terms of the fracture stress σ_f

$$G_c = \frac{\sigma_f^2 \pi a}{E} \quad \text{in plane stress} \quad (11.33)$$

$$G_c = \frac{\sigma_f^2 \pi a}{E} (1 - \nu^2) \quad \text{in plane strain.} \quad (11.34)$$

For finite bodies and those with edge cracks, correction factors must be introduced. Usually this involves replacing the factor π by some dimensionless function of the cracked body's geometry.

From eqns. (11.32) and (11.34) we can predict that, *for plane strain*, the fracture stress should be given by

$$\sigma_f^2 = \frac{2bE\gamma}{\pi a(1 - \nu^2)} \quad (11.35)$$

or, *for plane stress*:

$$\sigma_f^2 = \frac{2bE\gamma}{\pi a}$$

Griffith tested his theory on inorganic glasses and found a reasonable correlation between predicted and observed values of fracture stress. However, inorganic glasses are extremely brittle and when more ductile materials are examined it is found that the predicted values are far less than those observed. It is now known that even in apparently brittle fractures a ductile material will produce a localised plastic zone at the crack tip which effectively

blunts the crack. This has not prevented some workers measuring G_c experimentally and using it as a means of comparing materials but it is then understood that the energy required to propagate the crack includes the energy to produce the plastic zone.

(b) Stress intensity factor

Griffith's criterion is an energy-based theory which ignores the actual stress distribution near the crack tip. In this respect the theory is somewhat inflexible. An alternative treatment of the elastic crack was developed by Irwin⁽¹⁶⁾, who used a similar mathematical model to that employed by Griffith except in this case the remotely applied stress is biaxial – (see Fig. 11.37). Irwin's theory obtained expressions for the stress components near the crack tip. The most elegant expression of the stress field is obtained by relating the cartesian components of stress to polar coordinates based at the crack tip as shown in Fig. 11.38.

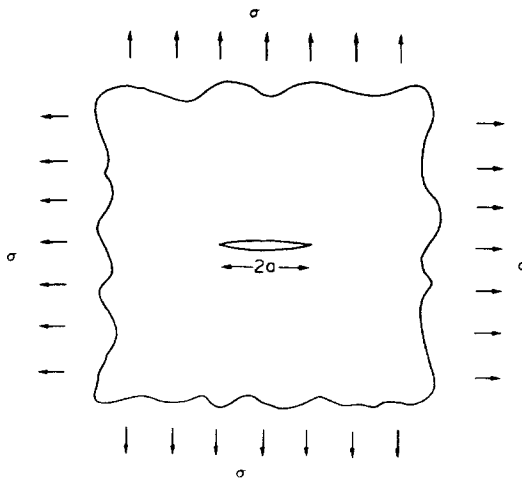


Fig. 11.37. Mathematical model for Irwin's analysis.

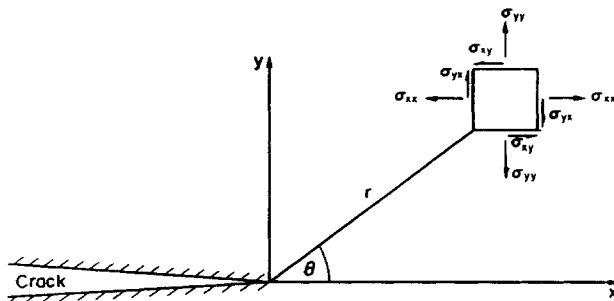


Fig. 11.38. Coordinate system for stress components in Irwin's analysis.

Then we have:

$$\left. \begin{aligned} \sigma_{yy} &= \frac{K}{\sqrt{2\pi r}} \cos \frac{\theta}{2} \left[1 + \sin \frac{\theta}{2} \sin \frac{3\theta}{2} \right] \\ \sigma_{xx} &= \frac{K}{\sqrt{2\pi r}} \cos \frac{\theta}{2} \left[1 - \sin \frac{\theta}{2} \sin \frac{3\theta}{2} \right] \\ \sigma_{xy} &= \frac{K}{\sqrt{2\pi r}} \cos \frac{\theta}{2} \sin \frac{\theta}{2} \cos \frac{3\theta}{2} \end{aligned} \right\} \quad (11.36)$$

With, for plane stress,

$$\sigma_{zz} = 0$$

or, for plane strain,

$$\sigma_{zz} = \nu(\sigma_{xx} + \sigma_{yy})$$

with

$$\sigma_{zx} = \sigma_{zy} = 0 \quad \text{for both cases.}$$

The expressions on the right-hand side of the above equations are the first terms in series expansions but for regions near the crack tip where $r/a \gg 1$ the other terms can be neglected.

It is evident that each stress component is a function of the parameter K and the polar coordinates determining the point of measurement. The parameter K , which is termed the “*stress intensity factor*”, therefore uniquely determines the stress field near the crack tip. If we base our criterion for fracture on the stresses near the crack tip then we are implying that the value of K determines whether the crack will propagate or not. The stress intensity factor K is simply a function of the remotely applied stress and crack length.

If more than one crack opening mode is to be considered then K sometimes carries the suffix I, II or III corresponding to the three modes shown in Fig. 11.34. However since this text is restricted to consideration of mode I crack propagation only, the formulae have been simplified by adopting the symbol K without its suffix. Other texts may use the full symbol K_I in development of similar formulae.

For Irwin’s model, K is given by

$$K = \sigma\sqrt{\pi a} \quad (11.37a)$$

For an edge crack in a semi-infinite sheet

$$K = 1.12\sigma\sqrt{\pi a} \quad (11.37b)$$

To accommodate different crack geometries a flaw shape parameter Q is sometimes introduced thus

$$K = \sigma\sqrt{\frac{\pi a}{Q}} \quad (11.37c)$$

or, for an edge crack

$$K = 1.12\sigma\sqrt{\frac{\pi a}{Q}} \quad (11.37d)$$

Values of Q for various aspect (depth to width) ratios of crack can be obtained from standard texts*, but, typically, they range from 1.0 for an aspect ratio of zero to 2.0 for an aspect ratio of 0.4.

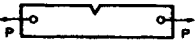
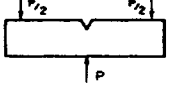
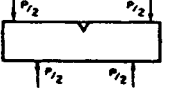
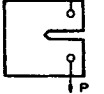
* Knott and Elliot, *Worked Examples in Fracture Mechanics*, Inst. met.

Normal manufactured components are of finite size and generally cracks grow from a free surface. However, for regions near the crack tip it is found that eqn (11.36) is a good approximation to the stress field if the stress intensity factor is modified to

$$K = \sigma Y \sqrt{a} \tag{11.38}$$

where a is the length of the edge crack and Y is a dimensionless correction factor often termed a “compliance function”. Y is a polynomial of the ratio a/W where W is the uncracked width in the crack plane (see Table 11.1).

Table 11.1. Table of compliance functions (Y).

Compliance function $Y = A \left(\frac{a}{W}\right)^{1/2} - B \left(\frac{a}{W}\right)^{3/2} + C \left(\frac{a}{W}\right)^{5/2} - D \left(\frac{a}{W}\right)^{7/2} + E \left(\frac{a}{W}\right)^{9/2}$ with W = uncracked specimen width; a = length of edge crack; b = specimen thickness; P = total load; L = distance between loading points							
Specimen geometry	Specimen nomenclature	Equation for K	Compliance function constants				
			A	B	C	D	E
	Single edge notched (S.E.N.)	$K = \frac{P}{bW^{1/2}} \cdot Y$	1.99	0.41	18.70	38.48	53.85
	Three-point bend ($L = 4W$)	$K = \frac{3PL}{bW^{3/2}} \cdot Y$	1.93	3.07	14.53	25.11	25.80
	Four-point bend	$K = \frac{3PL}{bW^{3/2}} \cdot Y$	1.99	2.47	12.97	23.17	24.80
	Compact tension (C.T.S.)	$K = \frac{P}{bW^{1/2}} \cdot Y$	29.60	185.50	655.70	1017.0	638.90

It is common practice to express K in the directly measurable quantities of load P , thickness b , and width W . The effect of crack length is then totally incorporated into Y .

i.e.
$$K = \frac{P}{bW^{1/2}} \cdot Y \tag{11.39}$$

In practice, values of K can be determined for any geometry and for different types of loading. Table 11.1 gives the expressions derived for common laboratory specimen geometries.

Photoelastic determination of stress intensity factors

The stress intensity factor K defined in §11.3.2 is an important and useful parameter because it uniquely describes the stress field around a crack tip under tension. In a two-dimensional system the stress field around the crack tip has been defined, in polar co-ordinates, by eqns. (11.36) as

$$\left. \begin{aligned} \sigma_{xx} &= \frac{K}{\sqrt{2\pi r}} \cos \frac{\theta}{2} \left[1 - \sin \frac{\theta}{2} \sin \frac{3\theta}{2} \right] \\ \sigma_{yy} &= \frac{K}{\sqrt{2\pi r}} \cos \frac{\theta}{2} \left[1 + \sin \frac{\theta}{2} \sin \frac{3\theta}{2} \right] \\ \tau_{xy} &= \frac{K}{\sqrt{2\pi r}} \cos \frac{\theta}{2} \sin \frac{\theta}{2} \cos \frac{3\theta}{2} \end{aligned} \right\} \quad (11.36)\text{bis}$$

with the crack plane running along the line $\theta = \pi$, see Fig. 11.38.

From §6.15 photoelastic fringes or “isochromatics” are contours of equal maximum shear stress τ_{\max} and from Mohr circle proportions, or from eqn. (13.13),[†]

$$\tau_{\max} = \frac{1}{2} \sqrt{(\sigma_{xx} - \sigma_{yy})^2 + 4\tau_{xy}^2}$$

Substituting eqns. (11.36) gives

$$\tau_{\max} = \frac{K \sin \theta}{2\sqrt{2\pi r}} \quad (11.40)$$

If, therefore, a photoelastic model is constructed of the particular crack geometry under consideration (see Fig. 11.39) a plot of τ_{\max} against $1/\sqrt{r}$ from the crack tip will produce a straight line graph from the slope of which K can be evaluated.

It is usual to record fringe order (and hence τ_{\max} values) along the line $\theta = 90^\circ$ when r will be at a maximum r_{\max} . Then:

$$\tau_{\max} = \frac{K}{2\sqrt{2\pi}} \cdot \frac{1}{\sqrt{r_{\max}}}$$

i.e.
$$\text{slope of graph} = \frac{K}{2\sqrt{2\pi}}$$

Correction factors

Equations (11.36), above, were derived for mathematical convenience for an infinite sheet containing a central crack of length $2a$ loaded under biaxial tension. For these conditions it is found that

$$K = \sigma\sqrt{\pi a}$$

In order to allow for the fact that the loading in the photoelastic test is uniaxial and that the model is of finite, limited size, a correction factor needs to be applied to the above K value in order that the “theoretical” value can be obtained and compared with the result obtained from the photoelastic test. This is normally written in terms of the function (a/w) where a = edge crack length and w = plate width. Then:

$$K = \sigma\sqrt{a} \left[1.99 - 0.41 \left(\frac{a}{w} \right) + 18.7 \left(\frac{a}{w} \right)^2 - 38.48 \left(\frac{a}{w} \right)^3 + 53.85 \left(\frac{a}{w} \right)^4 \right]$$

[†] E.J. Hearn, *Mechanics of Materials 1*, Butterworth-Heinemann, 1997.

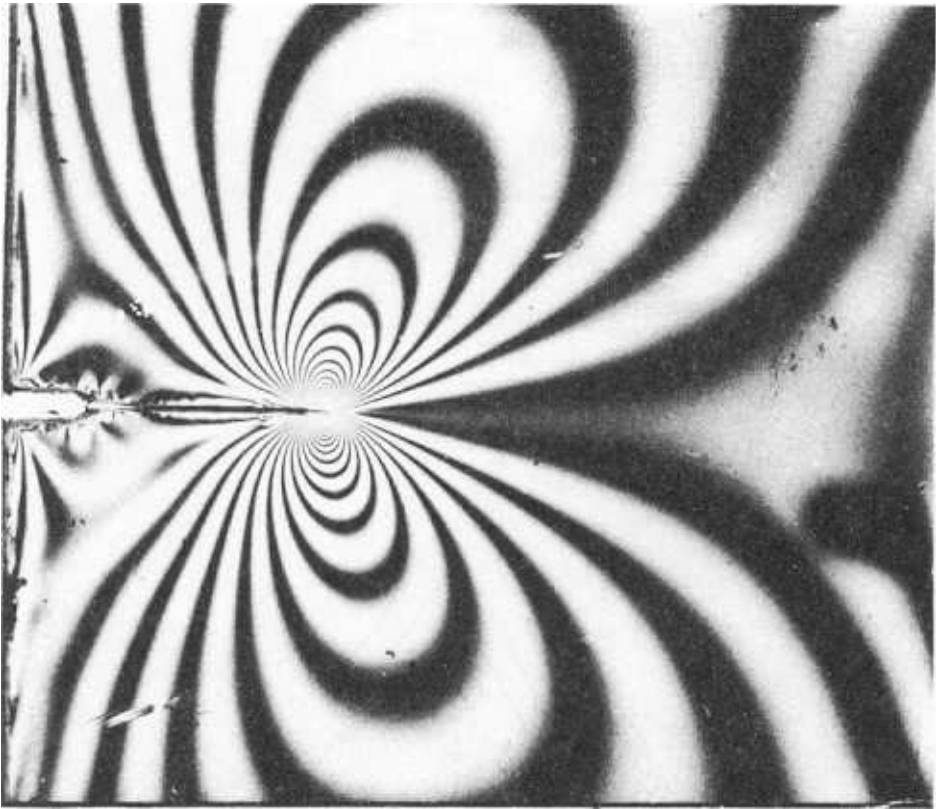


Fig. 11.39. Photoelastic fringe pattern associated with a particular crack geometry (relevant stress component nomenclature given in Fig. 11.38)

11.3.3. Elastic-plastic fracture mechanics (E.P.F.M.)

Irwin’s description of the stress components near an elastic crack can be summarised as

$$\text{Stress} \propto \frac{K}{r^{1/2}} \times \text{a function of } \theta - \text{ see eqn. } .36$$

which implies that each stress component rises to infinity as the crack tip is approached and as r nears zero.

In particular, the vertical stress in the crack plane where $\theta = 0$ is given by

$$\sigma_{yy} = \frac{K}{(2\pi x)^{1/2}} \tag{11.41}$$

which is represented by the dotted line shown in Fig. 11.40(a).

In a ductile material then, at some point the stress will exceed the yield stress and the material will yield. By following Knott’s analysis⁽¹⁷⁾ we can estimate the extent of the plastic deformation.

If we consider *plane stress conditions* then σ_{yy} is the maximum and σ_{zz} the minimum (= 0) principal stress. Then, by the Tresca criterion, the material will shear in the yz plane

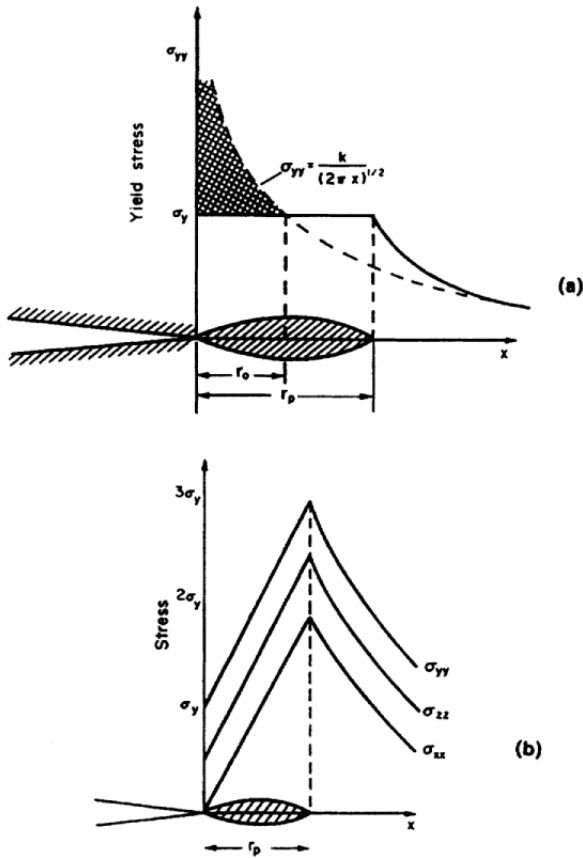


Fig. 11.40. Schematic representation of crack tip plasticity in; (a) plane stress; (b) plane strain.

and at 45° to the y and z axes when

$$\sigma_{yy} - \sigma_{zz} = \sigma_y$$

or

$$\sigma_{yy} = \sigma_y$$

where σ_y is the yield stress in uniaxial tension.

At some distance r_0 from the crack tip $\sigma_{yy} = \sigma_y$ as shown in Fig. 11.40(a). By simple integration, the area under the curve between the crack tip and r_0 is equal to $2\sigma_y r_0$. The shaded area in the figure must therefore have an area $\sigma_y r_0$. It is conventional to assume that the higher stress levels associated with the shaded area are redistributed so that the static zone extends a distance r_p where

$$r_p = 2r_0 = \frac{K^2}{\pi\sigma_y^2} \tag{11.42}$$

Figure 11.40(a) shows the behaviour of $\sigma_{yy}(x, 0)$, i.e. the variation of σ_{yy} with x at $y = 0$, for the case of plane stress. This is only a first approximation, but the estimate of the plastic zone size differs only by a small numerical factor from refined treatments. *In the case of plane strain* σ_{zz} is non-zero and σ_{xx} is the smallest principal stress in the vicinity of the

crack tip. Again, by using the Tresca criterion, we have

$$\sigma_{yy} - \sigma_{xx} = \sigma_y$$

or

$$\sigma_{yy} = \sigma_y + \sigma_{xx}$$

In the plastic zone the difference between σ_{yy} and σ_{xx} must be maintained at σ_y . As x increases from the crack tip σ_{xx} rises from zero and so σ_{yy} must rise above σ_y . The normal stress σ_{zz} must also increase and a schematic representation is shown in Fig. 11.40(b). The stress configuration is one of triaxial tension and the constraints on the material produce stresses higher than the uniaxial yield stress. The maximum stress under these conditions is often conveniently taken to be $3\sigma_y$. The plane strain plastic zone size is therefore taken to be one-third of the plane stress plastic zone

$$\text{i.e.} \quad r_p = \frac{K^2}{3\pi\sigma_y^2} \quad (11.43)$$

In both states of stress it is seen that the square of the stress intensity factor determines the size of the plastic zone. This would seem paradoxical as K is derived from a perfectly elastic model. However, if the plastic zone is small, the elastic stress field in the region around the plastic zone will still be described by eqn. (11.43). The plasticity is then termed “well-contained” or “ K -controlled” and we have an *elastic-plastic stress distribution*. A typical criterion for well-contained plasticity is that the plastic zone size should be less than one-fiftieth of the uncracked specimen ligament.

11.3.4. Fracture toughness

A fracture criterion for brittle and elastic-plastic cracks can be based on functions of the elastic stress components near the crack tip. No matter what function is assumed it is implied that K reaches some critical value since each stress component is uniquely determined by K . In other words the crack will become unstable when K reaches a value K_{IC} , the *Critical stress intensity factor* in mode I. K_{IC} is now almost universally denoted as the “*fracture toughness*”, and is used extensively to classify and compare materials which fracture under plane strain conditions.

The fracture toughness is measured by increasing the load on a pre-cracked laboratory specimen which usually has one of the geometries shown in Table 11.1. When the onset of crack growth is detected then the load at that point is used to calculate K_{IC} .

In brittle materials, the onset of crack growth is generally followed by a catastrophic failure whereas ductile materials may withstand a period of stable crack growth before the final fracture. The start of the stable growth is usually detected by changes in the compliance of the specimen and a clip-gauge mounted across the mouth of the crack produces a sensitive method of detecting changes in compliance. It is important that the crack is sharp and that its length is known. In soft materials a razor edge may suffice, but in metals the crack is generally grown by fatigue from a machined notch. The crack length can be found after the final fracture by examining the fracture surfaces when the boundary between the two types of growth is usually visible. Typical values of the fracture toughness of some common materials are given in Table 11.2.

Table 11.2. Typical K_{IC} values.

Material	K_{IC} (MN/m ^{3/2})
Concrete (dependent on mix and void content)	0.1–0.15
Epoxy resin	0.5–2.0
Polymethylmethacrylate	2–3
Aluminium	20–30
Low alloy steel	40–60

11.3.5. Plane strain and plane stress fracture modes

Generally, in plane stress conditions, the plastic zone crack tip is produced by shear deformation through the thickness of the specimen. Such deformation is enhanced if the thickness of the specimen is reduced. If, however, the specimen thickness is increased then the additional constraint on through-thickness yielding produces a triaxial stress distribution so that approximate plane strain deformation occurs with shear in the xy plane. There is usually a transition from plane stress to plane strain conditions as the thickness is increased. As K_{IC} values are generally quoted for plane strain, it is important that this condition prevails during fracture toughness testing.

A well-established criterion for plane strain conditions is that the thickness B should obey the following:

$$B \geq 2.5 \frac{(K_{IC})^2}{\sigma_y^2} \quad (11.44)$$

It should be noted that, even on the thickest specimens, a region of plane stress yielding is always present on the side surfaces because no triaxial stress can exist there. The greater plasticity associated with the plane stress deformation produces the characteristic “*shear lips*” often seen on the edges of fracture surfaces. In some instances the plane stress regions on the surfaces may be comparable in size with nominally plane strain regions and a mixed-mode failure is observed. However, many materials show a definite transition from plane stress to plane strain.

11.3.6. General yielding fracture mechanics

When the extent of plasticity which accompanies the growth of a crack becomes comparable with the crack length and the specimen dimensions we cannot apply linear elastic fracture mechanics (LEFM) and other theories have to be sought. It is beyond the scope of this book to review all the possible attempts to provide a unified theory. We will, however, examine the J integral developed by Rice⁽¹⁸⁾ because this has found the greatest favour in recent years amongst researchers in this field. In its simplest form the J integral can be defined as

$$J = \frac{\partial U^*}{\partial a} \quad (11.45)$$

where the asterisk denotes that this energy release rate includes both linear elastic and non-linear elastic strain energies. For linear elasticity J is equivalent to G .

The theory of the J integral was developed for non-linear *elastic* behaviour but, in the absence of any rival theory, the J integral is also used when the extent of *plasticity* produces a non-linear force-displacement curve.

As the crack propagates and the crack tip passes an element of the material, the element will partially unload. In cases of general yielding the elements adjacent to the crack tip will have been plastically deformed and will not unload reversibly, and the strain energy released will not be as great as for reversible non-linear elastic behaviour. At the initiation of growth no elements will have unloaded so that if we are looking for a criterion for crack growth then the difference between plastic and nonlinear elastic deformation may not be significant. By analogy with Griffith's definition of G_c in eqn. (11.32) we can define

$$J_c = \left(\frac{\partial U^*}{\partial a} \right)_c \quad (11.46)$$

the critical strain energy release rate for crack growth. Here the energy required to extend the crack is dominated by the requirement to extend the plastic zone as the crack grows. The surface energy of the new crack faces is negligible in comparison. Experiments on mild steel⁽¹⁶⁾ show that J_c is reasonably constant for the initiation of crack growth in different specimen geometries.

Plastic deformation in many materials is a time-dependent process so that, at normal rates of loading, the growth of cracks through structures with gross yielding can be stable and may be arrested by removing the load.

Calculation of J

Several methods of calculating J exist, but the simplest method using normal laboratory equipment is that developed by Begley and Landes.⁽¹⁹⁾ Several similar specimens of any suitable geometry are notched or pre-cracked to various lengths. The specimens are then extended while the force-displacement curves are recorded. Two typical traces where the crack length a_2 is greater than a_1 are shown in Fig. 11.41. At any one displacement x , the area under the $W-x$ curve gives U^* . For any given displacement, a graph can be plotted of

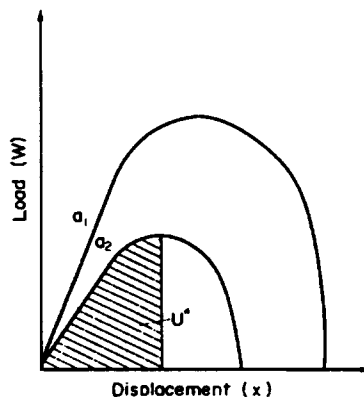


Fig. 11.41. Force-displacement curves for cracked bodies exhibiting general yielding (crack length $a_1 < a_2$)

U^* against crack length (Fig. 11.42). The slopes of these curves give J for any given combination of crack length and displacement, and can be plotted as a function of displacement (Fig. 11.43). By noting the displacement at the onset of crack growth, J_c can be assessed.

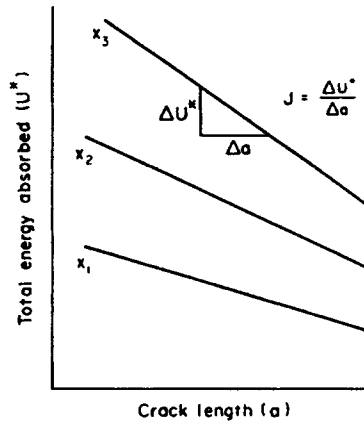


Fig. 11.42. Total energy absorbed as a function of crack length and at constant displacement ($x_3 > x_2 > x_1$)

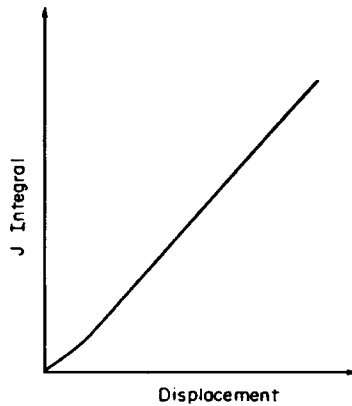


Fig. 11.43. The J integral as a function of displacement.

11.3.7. Fatigue crack growth

The failure of engineering components most commonly occurs at stress levels far below the maximum design stress. Also, components become apparently more likely to fail as their service life increases. This phenomenon, commonly termed fatigue, see §11.1, involves the growth of small defects into macroscopic cracks which grow until K_{IC} is exceeded and catastrophic failure occurs. One of the earliest observations of fatigue failure was that the amplitude of fluctuations in the applied stress had a greater influence on the fatigue life of

a component than the mean stress level. In fact if there is no fluctuation in loading then fatigue failure cannot occur, whatever magnitude of static stress is applied.

As stated earlier, fatigue failure is generally considered to be a three-stage process as shown schematically in Fig. 11.44. *Stage I* involves the initiation of a crack from a defect and the subsequent growth of the crack along some favourably orientated direction in the microstructure. Eventually the crack will become sufficiently large that the microstructure has a reduced effect on the crack direction and the crack will propagate on average in a plane normal to the maximum principal stress direction. This is *stage II* growth which has attracted the greatest attention because it is easier to quantify than the initiation stage. When the crack has grown so that K_{IC} is approached the crack accelerates more rapidly until K_{IC} is exceeded and a final catastrophic failure occurs. This accelerated growth is classified as *stage III*.

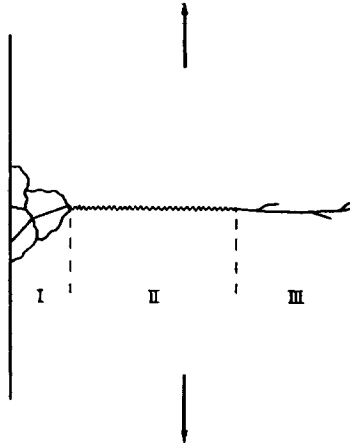


Fig. 11.44. Schematic representation of the three stages of fatigue crack growth.

The rate of growth of a fatigue crack is described in terms of the increase in crack length per load cycle, da/dN . This is related to the amplitude of the stress intensity factor, ΔK , during the cycle. If the amplitude of the applied stress remains constant then, as the crack grows, ΔK will increase. Such conditions produce growth-rate curves of the type shown in Fig. 11.45. Three distinct sections, which corresponds to the three stages of growth, can be seen.

There is a minimum value of ΔK below which the crack will not propagate. This is termed the *threshold value* or ΔK_{th} and is usually determined when the growth rate falls below 10^{-7} mm/cycle or, roughly, one atomic spacing. Growth rates of 10^{-9} mm/cycle can be detected but at this point we are measuring the average increase produced by a few areas of localised growth over the whole crack front. To remove any possibility of fatigue failure in a component it would be necessary to determine the maximum defect size, assume it was a sharp crack, and then ensure that variations in load do not produce ΔK_{th} .

Usually this would result in an over-strong component and it is necessary in many applications to assume that some fatigue crack growth will take place and assess the lifetime of the component before failure can occur. Only sophisticated detection techniques can resolve

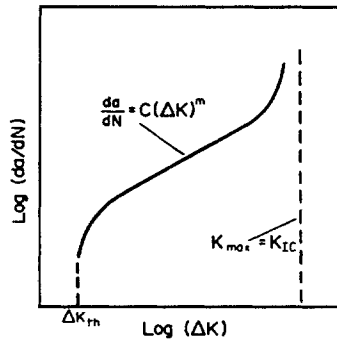


Fig. 11.45. Idealised crack growth rate plot for a constant load amplitude.

cracks in the initiation stage and generally it is assumed that the lifetime of fatigue cracks is the number of cycles endured in stage II.

For many materials stage II growth is described by the *Paris–Erdogan Law*⁽²⁰⁾.

$$\frac{da}{dN} = C(\Delta K)^m \quad (11.47)$$

C and m are material coefficients. Usually m lies between 2 and 7 but values close to 4 are generally found. This simple relationship can be used to predict the lifetime of a component if the stress amplitude remains approximately constant and the maximum crack size is known. If the stress amplitude varies, then the growth rate may depart markedly from the simple power law. Complications such as fatigue crack closure (effectively the wedging open of the crack faces by irregularities on the crack faces) and single overloads can reduce the crack growth rate drastically. Small changes in the concentration of corrosive agents in the environment can also produce very different results.

Stage III growth is usually a small fraction of the total lifetime of a fatigue crack and often neglected in the assessment of the maximum number of load cycles.

Since we are considering ΔK as the controlling parameter, only brittle materials or those with well-contained plasticity can be treated in this manner. When the plastic deformation becomes extensive we need another parameter. Attempts have been made to fit growth-rate curves to ΔJ the amplitude of the J integral. However while non-linear elastic and plastic behaviour may be conveniently merged in monotonic loading, in cyclic loading there are large differences in the two types of deformation. The non-linear elastic material has a reversible stress–strain relationship, while large hysteresis is seen when plastic material is stressed in the opposite sense. As yet the use of ΔJ has not been universally accepted but, on the other hand, no other suitable parameter has been developed.

11.3.8. Crack tip plasticity under fatigue loading

As a cracked body is loaded, a plastic zone will grow at the crack tip as described in §11.3.3. When the maximum load is reached and the load is subsequently decreased, the deformation of the plastic zone will not be entirely reversible. The elastic regions surrounding the plastic zone will attempt to return to their original displacement as the load is reduced. However, the plastic zone will act as a type of inclusion which the relaxing elastic material

then loads in compression. The greatest plastic strain on the increasing part of the load cycle is near the crack tip, and is therefore subjected to the lightest compressive stresses when the load decreases. At a sufficiently high load amplitude the material near the crack tip will yield in compression. A “reverse” plastic zone is produced inside the material which has previously yielded in tension. Figure 11.46 shows schematically the configuration of crack tip plasticity and the variation in vertical stress, in plane stress conditions, at the minimum load of the load cycle.

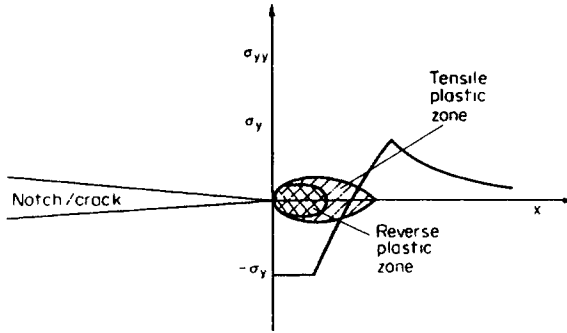


Fig. 11.46. Crack tip plasticity at the minimum load of the load cycle (plane stress conditions)

The material adjacent to the crack tip is therefore subjected to alternating plastic strains which lead to cumulative plastic damage and a weakening of the structure so that the crack can propagate. In metallic materials, striations on the fracture surface show the discontinuous nature of the crack propagation, and in many cases it can be assumed that the crack grows to produce a striation during each load cycle. Polymeric materials, however, can only show striations which occur after several thousands of load cycles.

11.3.9 Measurement of fatigue crack growth

In order to evaluate the fatigue properties of materials SN curves can be constructed as described in §11.1.1, or growth-rate curves drawn as shown in Fig. 11.45. Whilst non-destructive testing techniques can be used to detect fatigue cracks, e.g. ultrasonic detection methods to find flaws above a certain size or acoustic emission to determine whether cracks are propagating, growth-rate analysis requires more accurate measurement of crack length. Whilst a complete coverage of the many procedures available is beyond the scope of this text it is appropriate to introduce the most commonly used technique for metal fatigue studies, namely the D.C. potential drop method.

Essentially a large constant current (~ 30 amps) is passed through the specimen. As the crack grows the potential field in the specimen is disturbed and this disturbance is detected by a pair of potential probes, usually spot-welded on either side of the crack mouth. For single-edge notched (SEN) tensile and bend specimens theoretical solutions exist to relate the measured voltage to the crack length. In compact tension specimens (CTS) empirical calibrations are usually performed prior to the actual tests. Fig. 11.47 shows a block diagram of the potential drop technique. The bulk of the signal is “backed off” by the voltage source so that small changes in crack length can be detected. As the measured voltage is generally

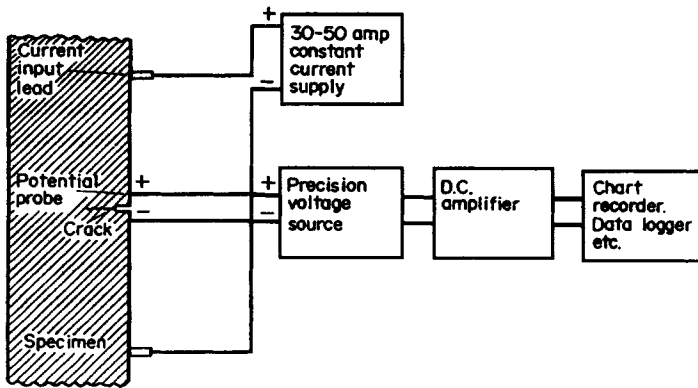


Fig. 11.47. Block diagram of the D.C. potential drop system for crack length measurement.

of the order of microvolts (steel and titanium) or nanovolts (aluminium), sensitive and stable amplifiers and voltage sources are required. A constant temperature environment is also desirable. If adequate precautions are taken, apparent increases in crack length of 10^{-9} mm can be detected in some materials.

If the material under test is found to be insensitive to loading frequency and a constant loading amplitude is required, the most suitable testing machine is probably one which employs a resonance principle. Whilst servo-hydraulic machines can force vibrations over a wider range of frequencies and produce intricate loading patterns, resonance machines are generally cheaper and require less maintenance. Each type of machine is usually provided with a cycle counter and an accurate load cell so that all the parameters necessary to generate the growth rate curve are readily available.

References

1. Goodman, J. *Mechanics Applied to Engineering*, vol. 1, 9th Ed. Longmans Green, 1930.
2. Gerber, W. "Bestimmung der zulässigen spannungen in eisen constructionen", *Z. Bayer Arch. Ing. Ver.*, 6 (1874).
3. Soderberg, C.R. "Factor of safety and working stresses" *Trans. ASME, J. App. Mech.*, 52 (1930).
4. Juvinall, R.C. *Engineering Considerations of Stress, Strain and Strength*. McGraw Hill, 1967.
5. Shigley, J.E. *Mechanical Engineering Design*, 3rd Edn. McGraw-Hill, 1977.
6. Osgood, C.C. *Fatigue Design*. 2nd Edn. Pergamon Press, 1982.
7. Miner, M.A. "Cumulative damage in fatigue", *Trans. ASME*, 67 (1945).
8. Coffin, L.F. Jr. "Low cycle fatigue: a review", General Electric Research Laboratory, Reprint No. 4375, Schenectady, N.W., October 1962.
9. Basquin, H.O. "The exponential law of endurance tests", *Proc. ASTM*, 10 (1910).
10. Forsyth, P.J.E. *J. Inst. Metals*, 82 (1953).
11. Cottrell, A.H. and Hull, D. *Proc. Roy. Soc. A* 242 (1957).
12. Larson, F.R. and Miller, J. "A time-temperature relationship for rupture and creep stress", *Trans ASME*, 74 (1952).
13. Manson, S.S. and Haferd, A.M. "A linear time-temperature relation for extrapolation of creep and stress-rupture data", *NACA Tech. Note* 2890 (1953).
14. Orr, R.L., Sherby, O.D. and Dorn, J.E. "Correlation of rupture data for metals at elevated temperatures", *Trans ASME*, 46 (1954).
15. Griffith, A.A. *Proc. Roy. Soc., A*, 221 (1920).
16. Irwin, G.R. *J. Appl. Mech. Trans. ASME*, 24 (1957), 361.
17. Knott, J.F. *Fundamentals of Fracture Mechanics*. Butterworths, 1973.

18. Rice, J.R. *J. Appl. Mech. Trans. ASME*, **35** (1968), 379.
19. Begley, J.A. and Landes, D. *The J Integral as a Fracture Criterion*. ASTM STP 514 (1972).
20. Paris, P. and Erdogan, F. *J. Basic. Eng.*, **85** (1963), 265.

Examples

Example 11.1

The fatigue behaviour of a specimen under alternating stress conditions with zero mean stress is given by the expression:

$$\sigma_r^a \cdot N_f = K$$

where σ_r is the range of cyclic stress, N_f is the number of cycles to failure and K and a are material constants.

It is known that $N_f = 10^6$ when $\sigma_r = 300 \text{ MN/m}^2$ and $N_f = 10^8$ when $\sigma_r = 200 \text{ MN/m}^2$.

Calculate the constants K and a and hence the life of the specimen when subjected to a stress range of 100 MN/m^2 .

Solution

Taking logarithms of the given expression we have:

$$a \log \sigma_r + \log N_f = \log K \tag{1}$$

Substituting the two given sets of condition for N_f and σ_r :

$$2.4771a + 6.0000 = \log K \tag{2}$$

$$2.3010a + 8.0000 = \log K \tag{3}$$

$$\therefore (3) - (2) \qquad \qquad \qquad -0.1761a + 2.0000 = 0$$

$$a = \frac{2.0000}{0.1761} = 11.357$$

Substituting in eqn. (2)

$$11.357 \times 2.4771 + 6.000 = \log K = 34.1324$$

$$\therefore K = 1.356 \times 10^{33}$$

Hence, for stress range of 100 MN/m^2 , from eqn (1):

$$11.357 \times 2.0000 + \log N_f = 34.1324$$

$$22.714 + \log N_f = 34.1324$$

$$\log N_f = 11.4184$$

$$N_f = 262.0 \times 10^9 \text{ cycles}$$

Example 11.2

A steel bolt 0.003 m^2 in cross-section is subjected to a static mean load of 178 kN. What value of completely reversed direct fatigue load will produce failure in 10^7 cycles? Use the Soderberg relationship and assume that the yield strength of the steel is 344 MN/m^2 and the stress required to produce failure at 10^7 cycles under zero mean stress conditions is 276 MN/m^2 .

Solution

From eqn. (11.9) of Soderberg

$$\sigma_a = \sigma_N \left[1 - \left(\frac{\sigma_m}{\sigma_y} \right) \right]$$

$$\begin{aligned} \text{Now, mean stress } \sigma_m \text{ on bolt} &= \frac{178 \times 10^{-3}}{3 \times 10^{-3}} \\ &= 59.33 \text{ MN/m}^2 \end{aligned}$$

$$\begin{aligned} \therefore \sigma_a &= 276 \left(1 - \frac{59.33}{344} \right) \\ &= 276(1 - 0.172) \\ &= 276 \times 0.828 \\ &= 228.5 \text{ MN/m}^2 \end{aligned}$$

$$\begin{aligned} \therefore \text{Load} &= 228.5 \times 0.003 \text{ MN} \\ &= 0.6855 \text{ MN} \\ &= \mathbf{685.5 \text{ kN}} \end{aligned}$$

Example 11.3

A stepped steel rod, the smaller section of which is 50 mm in diameter, is subjected to a fluctuating direct axial load which varies from +178 kN to -178 kN.

If the theoretical stress concentration due to the reduction in section is 2.2, the notch sensitivity factor is 0.97, the yield strength of the material is 578 MN/m^2 and the fatigue limit under rotating bending is 347 MN/m^2 , calculate the factor of safety if the fatigue limit in tension-compression is 0.85 of that in rotating bending.

Solution

From eqn. (11.12)

$$q = \frac{K_f - 1}{K_t - 1}$$

$$\begin{aligned} \therefore K_f &= q(K_t - 1) + 1 \\ &= 0.97(2.2 - 1) + 1 \\ &= 2.16 \end{aligned}$$

But
$$\begin{aligned}\sigma_{\max} &= \frac{178 \times 4}{\pi \times (0.05)^2} \\ &= 90642 \text{ kN/m}^2 \\ &= \mathbf{90.64 \text{ MN/m}^2}\end{aligned}$$

$\therefore \sigma_{\min} = -90.64 \text{ MN/m}^2$ and $\sigma_{\text{mean}} = 0$

\therefore Under direct stress conditions

$$\begin{aligned}\sigma_N &= 0.85 \times 347 \\ &= \mathbf{294.95 \text{ MN/m}^2}\end{aligned}$$

From eqn. (11.13)

$$\sigma_a = \frac{\sigma_N}{K_f F} \left(1 - \frac{\sigma_m \times F}{\sigma_y} \right)$$

\therefore With common units of MN/m^2 :

$$90.64 = \frac{294.95}{2.16 \times F} \left(1 - \frac{0 \times F}{578} \right)$$

$$\begin{aligned}\therefore F &= \frac{294.95}{2.16 \times 90.64} \\ \mathbf{F} &= \mathbf{1.5}\end{aligned}$$

Example 11.4

The values of the endurance limits at various stress amplitude levels for low-alloy constructional steel fatigue specimens are given below:

σ_a (MN/m^2)	N_f (cycles)
550	1 500
510	10 050
480	20 800
450	50 500
410	1 25 000
380	2 75 000

A similar specimen is subjected to the following programme of cycles at the stress amplitudes stated; 3 000 at 510 MN/m^2 , 12 000 at 450 MN/m^2 and 80 000 at 380 MN/m^2 , after which the sample remained unbroken. How many additional cycles would the specimen withstand at 480 MN/m^2 prior to failure? Assume zero mean stress conditions.

Solution

From Miner's Rule, eqn. (11.14), with X the required number of cycles:

$$\begin{aligned}\frac{n_1}{N_1} + \frac{n_2}{N_2} + \frac{n_3}{N_3} + \dots \text{ etc} &= 1. \\ \therefore \frac{3\,000}{10\,050} + \frac{12\,000}{50\,500} + \frac{80\,000}{275\,000} + \frac{X}{20\,800} &= 1\end{aligned}$$

$$0.2985 + 0.2376 + 0.2909 + \frac{X}{20\,800} = 1$$

$$\frac{X}{20\,800} = 1 - 0.8270$$

$$\therefore X = 3598 \text{ cycles.}$$

Example 11.5

The blades in a steam turbine are 200 mm long and they elastically extend in operation by 0.02 mm. If the initial clearance between the blade tip and the housing is 0.075 mm and it is required that the final clearance be not less than 0.025 mm, calculate:

- (i) the maximum percentage creep strain that can be allowed in the blades,
- (ii) the minimum creep strain rate if the blades are to operate for 10 000 hours before replacement.

Solution

$$\begin{aligned} \text{Permissible creep extension} &= \text{Initial clearance} - (\text{Final clearance} + \text{Elastic extension}) \\ &= 0.075 - (0.025 + 0.02) \\ &= 0.03 \text{ mm} \\ \therefore \text{Max. percentage creep strain} &= \frac{0.03}{200} \times 100 \\ &= \mathbf{0.015\%} \\ \therefore \text{Min. creep rate} &= \frac{0.015}{10\,000} = \mathbf{1.5 \times 10^{-6} \% / h.} \end{aligned}$$

Example 11.6

The following secondary creep strain rates were obtained when samples of lead were subjected to a constant stress of 1.3 MN/m².

Temperature (°C)	Minimum creep rate (ϵ_s^0) (s ⁻¹)
33	8.71×10^{-5}
29	4.98×10^{-5}
27	3.42×10^{-5}

Assuming that the material complies with the Arrhenius equation, calculate the activation energy for creep of lead. Molar gas constant, $R = 8.314 \text{ J/mol K}$.

Solution

Construct a table as shown below:

°C	K	$\frac{1}{T} \times 10^{-3}$	ϵ_s^0	$\ln \epsilon_s^0$
33	306	3.27	8.71×10^{-5}	-9.3485
29	302	3.31	4.98×10^{-5}	-9.9156
27	300	3.33	3.42×10^{-5}	-10.2833

The creep rate is related to temperature by eqn. (11.19):

$$\epsilon_s^0 = Ae^{-H/RT}$$

Hence we can plot $\ln \epsilon_s^0$ against $\frac{1}{T}$ (as in Fig. 11.48)

From the graph.

$$\text{Slope} = 15.48 \times 10^3$$

But $H = \text{slope} \times R$

$$\therefore H = 15.48 \times 10^3 \times 8.314$$

$$= 128.7 \text{ kJ/mol.}$$

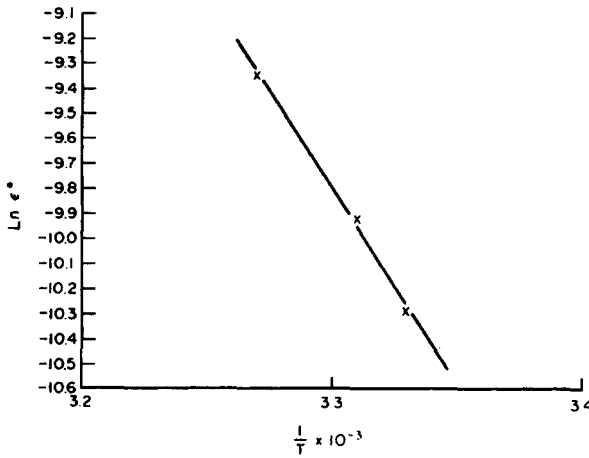


Fig. 11.48.

Example 11.7

An alloy steel bar 1500 mm long and 2500 mm² in cross-sectional area is subjected to an axial tensile load of 8.9 kN at an operating temperature of 600°C. Determine the value of creep elongation in 10 years using the relationship $\epsilon_s^0 = \beta \sigma^n$ if, for 600°C, $\beta = 26 \times 10^{-12} \text{ h}^{-1}(\text{N/mm}^2)^{-6}$, and $n = 6.0$.

Solution

$$\text{Applied stress } \sigma = \frac{P}{A} = \frac{8900}{2500} = 3.56 \text{ N/mm}^2$$

$$\text{Duration of test} = 10 \times 365 \times 24 = 87\,600 \text{ hours}$$

\therefore From eqn. (11.20)

$$\begin{aligned} \therefore \epsilon &= 26 \times 10^{-12} \times 87\,600 \times (3.56)^6 \\ &= 26 \times 10^{-12} \times 87\,600 \times 2036 \\ &= 4.637 \times 10^{-3} \end{aligned}$$

Since the member is 1 500 mm long,

$$\text{total elongation} = 1500 \times 4.637 \times 10^{-3} = \mathbf{6.96 \text{ mm.}}$$

Example 11.8

Creep tests carried out on an alloy steel at 600°C produced the following data:

Stress (kN/m ²)	Minimum creep rate (% / 10 000 h)
10.2	0.4
13.8	1.2
25.5	10.0

A rod, 150 mm long and 625 mm² in cross-section, made of a similar steel and operating at 600°C, is not to creep more than 3.2 mm in 10 000 hours. Calculate the maximum axial load which can be applied.

Solution

$$\% \text{ Creep strain} = \frac{3.2}{150} \times 100 = 2.13\% / 10\,000 \text{ h}$$

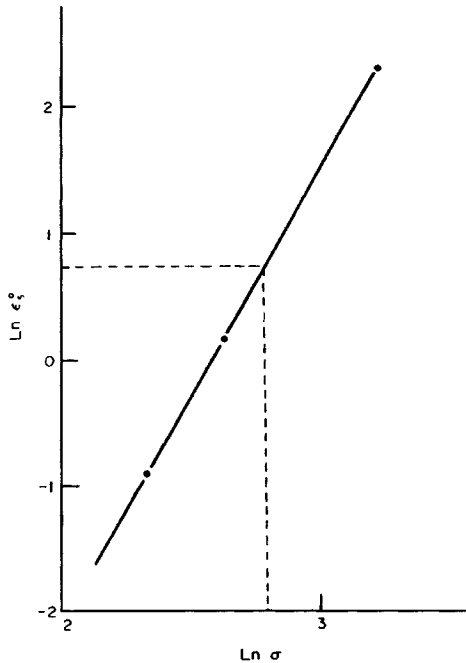


Fig. 11.49.

Since secondary creep rate is related to stress by the eqn. (11.20):

$$\epsilon_s^0 = \beta \sigma^n,$$

a graph may be plotted of $l_n \epsilon_s^0$ against $l_n \sigma$.

From the given data:

l_n stress	$l_n \epsilon_s^0$
2.3224	-0.9163
2.6247	0.1823
3.2387	2.3026

Producing the straight line graph of Fig. 11.49.

For % creep strain rate 2.13%, $l_n \epsilon_s^0 = 0.7561$.

∴ From graph, $l_n \sigma = 2.78$ and $\sigma = 16.12 \text{ kN/m}^2$.

If the cross sectional area of the rod is 625 mm^2

then $\text{load} = 16\,120 \times 625 \times 10^{-6}$
 $= 10 \text{ N}.$

Example 11.9

The lives of Nimonic 90 turbine blades tested under varying conditions of stress and temperature are set out in the table below.

Stress (MN/m ²)	Temperature (°C)	Life (h)
180	750	3 000
180	800	500
300	700	5 235
350	650	23 820

Use the information given to produce a master curve based upon the Larson–Miller parameter, and thus calculate the expected life of a blade when subjected to a stress of 250 MN/m^2 and a temperature of 750°C .

Solution

(i) To calculate C: from eqn. (11.23), inserting absolute temperatures:

$$T_1(l_n t_r + C) = T_2(l_n t_r + C)$$

$$1023(l_n 3000 + C) = 1073(l_n 500 + C)$$

$$1023(8.0064 + C) = 1073(6.2146 + C)$$

$$8190.5 + 1023C = 6668.27 + 1073C$$

$$1522.23 = 50C$$

$$C = 30.44.$$

(ii) To determine P values

Again, from eqn. (11.23):

$$\begin{aligned} P_1 &= [T(l_n t_r + C)] \\ &= 1023(l_n 3000 + 30.44) \\ &= \mathbf{39\ 330} \end{aligned}$$

$$\begin{aligned} P_2 &= 1073(l_n 500 + 30.44) \\ &= 1073(6.2146 + 30.44) \\ &= \mathbf{39\ 330} \end{aligned}$$

$$\begin{aligned} P_3 &= 973(l_n 5235 + 30.44) \\ &= 973(8.5632 + 30.44) \\ &= \mathbf{37\ 950} \end{aligned}$$

$$\begin{aligned} P_4 &= 923(l_n 23\ 820 + 30.44) \\ &= 923(10.0783 + 30.44) \\ &= \mathbf{37\ 398.} \end{aligned}$$

Plotting the master curve as per Fig. 11.31 we have the graph shown in Fig. 11.50.

From Fig. 11.50, when the stress equals 250 MN/m^2 the appropriate parameter $P = 38\ 525$
 \therefore For the required temperature of 750°C ($= 1023^\circ$ absolute)

$$38\ 525 = 1023(l_n t_r + 30.44)$$

$$38\ 525 = 1023 l_n t_r + 31\ 144$$

$$l_n t_r = 7.219$$

$$t_r = \mathbf{1365\text{ hours.}}$$

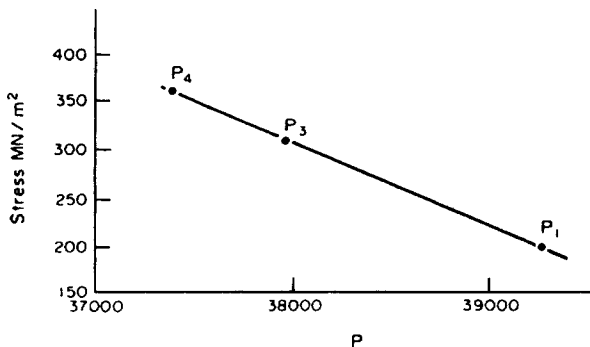


Fig. 11.50.

Example 11.10

The secondary creep rate in many metals may be represented by the equation

$$\dot{\varepsilon}^0 = \beta\sigma^n.$$

A steel bolt clamping two rigid plates together is held at a temperature of 1000°C. If n is 3.0 and $\dot{\varepsilon}^0 = 0.7 \times 10^{-9} \text{h}^{-1}$ at 28 MN/m², calculate the stress remaining in the bolt after 9000 h if the bolt is initially tightened to a stress of 70 MN/m².

Solution

$$\begin{aligned} \text{From eqn. (11.20)} \quad \dot{\varepsilon}^0 &= \beta\sigma^n \\ \therefore \quad 0.7 \times 10^{-9} &= \beta(28 \times 10^6)^3 \\ \therefore \quad \beta &= \frac{0.7 \times 10^{-9}}{21\,952 \times 10^{18}} \\ &= 3.189 \times 10^{-32} \end{aligned}$$

Using eqn. (11.27) for stress relaxation

$$\begin{aligned} \frac{1}{\sigma^{n-1}} &= \frac{1}{\sigma_i^{n-1}} + \beta E(n-1)t \\ \therefore \quad \frac{1}{\sigma^2} &= \frac{1}{(70 \times 10^6)^2} + 3.189 \times 10^{-32} \times 200 \\ &\quad \times 10^9 \times 2 \times 900 \\ \frac{1}{\sigma^2} &= 10^{-16} \times 3.188 \\ \sigma &= 10^8 \times \sqrt{\frac{1}{3.188}} \\ &= 10^8 \times 0.56 \\ \text{i.e. stress in bolt} &= \mathbf{56 \text{ MN/m}^2} \end{aligned}$$

Example 11.11

A steel tie in a girder bridge has a rectangular cross-section 200 mm wide and 20 mm deep.

Inspection reveals that a fatigue crack has grown from the shorter edge and in a direction approximately normal to the edge. The crack has grown 23 mm across the width on one face and 25 mm across the width on the opposite face.

If K_{IC} for the material is 55 MN/m^{3/2} estimate the greatest tension that the tie can withstand.

(Assume that the expression for K in a SEN specimen is applicable here.)

Solution

Since the crack length is not small compared with the width of the girder we need to calculate the compliance function.

$$\text{Hence} \quad a/W = 24/200 = 0.12$$

Then, from Table 11.1

$$\begin{aligned} Y &= 1.99(0.12)^{1/2} - 0.41(0.12)^{3/2} + 18.70(0.12)^{5/2} \\ &\quad - 38.48(0.12)^{7/2} + 53.85(0.12)^{9/2} \\ &= 0.689 - 0.017 + 0.093 - 0.023 + 0.004 \\ &= 0.745 \end{aligned}$$

Also, from eqn. (11.39),

$$K = \frac{PY}{BW^{1/2}}$$

At the onset of fracture $K = K_{IC}$

$$\therefore 55 \times 10^6 = \frac{P \times 0.745}{0.02 \times (0.2)^{1/2}}$$

Hence failure load $P = 660 \text{ kN}$.

Example 11.12

A thin cylinder has a diameter of 1.5 m and a wall thickness of 100 mm. The working internal pressure of the cylinder is 15 MN/m² and K_{IC} for the material is 38 MN/m^{3/2}. Estimate the size of the largest flaw that the cylinder can contain. (Assume that for this physical configuration $K = \sigma\sqrt{\pi a}$.)

Non-destructive testing reveals that no flaw above 10 mm exists in the cylinder. If, in the Paris–Erdogan formula, $C = 3 \times 10^{-12}$ (for K in MN/m^{3/2}) and $m = 3.8$, estimate the number of pressurisation cycles that the cylinder can safely withstand.

Solution

Assume that the flaw is sharp, of length $2a$, and perpendicular to the hoop stress.

Then from §9.1.1[†] hoop stress

$$\sigma = \frac{Pd}{2t} = \frac{15 \times 1.5}{2 \times 0.1} = 112.5 \text{ MN/m}^2$$

From eqn. (11.37a), at the point of fracture

$$K = K_{IC} = \sigma\sqrt{\pi a}$$

$$38 = 112.5\sqrt{\pi a}$$

Hence

$$a = 64.3 \text{ mm}$$

From eqn. (11.47)

$$\frac{da}{dN} = C(\Delta K)^m$$

and for pressurisation from zero $\Delta K = K_{\max}$

$$\therefore \frac{da}{\Delta K^m} = C \cdot dN$$

[†] E.J. Hearn, *Mechanics of Materials 1*, Butterworth-Heinemann, 1997.

$$\begin{aligned}
 N &= \frac{1}{C} \int_a^{a_{\max}} \frac{da}{(112.5\sqrt{\pi a})^{3.8}} \\
 &= 16.4 \left[\frac{-0.9}{a^{0.9}} \right]_{0.005}^{0.0643} \\
 &= 14.8(-11.88 + 1178) \\
 &= \mathbf{1156 \text{ cycles.}}
 \end{aligned}$$

Example 11.13

In a laboratory fatigue test on a CTS specimen of an aluminium alloy the following crack length measurements were taken.

Crack length (mm)	21.58	22.64	23.68	24.71	25.72	27.37	28.97	29.75
Cycles	3575	4255	4593	4831	5008	5273	5474	5514

The specimen has an effective width of 50.0 mm.

Load amplitude = 3 kN. Specimen thickness = 25.0 mm.

Construct a growth rate curve in order to estimate the constants *C* and *m* in the Paris–Erdogan equation

$$da/dN = C(\Delta K)^m$$

Use the expression given in Table 11.1 to evaluate ΔK .

Use the three-point method to evaluate da/dN .

i.e. at point *n*;

$$\left(\frac{da}{dN} \right)_n = \frac{a_{n+1} - a_{n-1}}{N_{n+1} - N_{n-1}}$$

Solution

Equation (11.47) gives the Paris–Erdogan law as

$$da/dN = C(\Delta K)^m$$

$$\log(da/dN) = \log C + m \log(\Delta K)$$

From Table 11.1 we can calculate the amplitude of the stress intensity factor from the equation

$$\begin{aligned}
 \Delta K &= \frac{\Delta P}{BW^{1/2}} \left[29.6 \left(\frac{a}{W} \right)^{1/2} - 185.5 \left(\frac{a}{W} \right)^{3/2} + 655.7 \left(\frac{a}{W} \right)^{5/2} \right. \\
 &\quad \left. - 1017 \left(\frac{a}{W} \right)^{7/2} + 638.9 \left(\frac{a}{W} \right)^{9/2} \right]
 \end{aligned}$$

The crack growth rate is most easily found by using the three-point method. The crack growth rate at the point *n* is calculated as the slope of the straight line joining the (*n* + 1)th and the (*n* – 1)th points.

i.e.
$$\left(\frac{da}{dN} \right)_n = \frac{a_{n+1} - a_{n-1}}{N_{n+1} - N_{n-1}}$$

From these calculations we obtain the following results

Crack length	21.58	22.64	23.68	24.71	25.72	27.37	28.97	29.75
Cycles	3575	4355	4593	4831	5008	5273	5474	5514
ΔK (MN/m ^{3/2})	4.13	4.38	4.65	4.84	5.26	5.86	6.57	6.97
$\log_{10}(\Delta K)$	0.616	0.642	0.668	0.685	0.721	0.769	0.818	0.843
$\frac{da}{dN} \times 10^6$ m/cycle		2.06	4.34	4.91	6.02	6.97	8.38	
$\log_{10}(da/dN)$		-5.68	-5.36	-5.31	-5.22	-5.15	-5.07	

A log-log plot of da/dN versus ΔK is shown in Fig. 11.51.

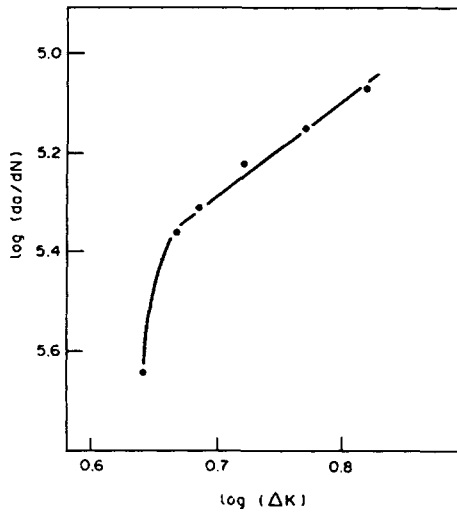


Fig. 11.51.

The first point is not close to the best straight line fit to the other points. The fatigue crack is normally initiated at a high stress amplitude in order to produce a uniform crack front. Although the stress amplitude is reduced gradually to the desired value the initial crack growth is through a crack tip plastic zone associated with the previous loading. The crack is then “blunted” by the larger plastic zone until the crack has grown through it. There is therefore a justification for ignoring this point.

A “least-squares” fit to the remaining points gives

$$\text{Slope} = 2.67 = m$$

$$\text{Intercept} = -7.57 = \log C$$

$$C = 2.69 \times 10^{-8}$$

The Paris-Erdogan equation (11.47) then becomes

$$\frac{da}{dN} = 2.69 \times 10^{-8} (\Delta K)^{2.67}$$

(For ΔK in MN/m^{3/2})

Problems

11.1 (B). (a) Write a short account of the microscopical aspects of fatigue crack initiation and growth.

(b) A fatigue crack is considered to have been initiated when the surface crack length has reached 10^{-3} mm. The percentage of cycle lifetime required to reach this stage may be calculated from the equation:

$$1000N_i = \sqrt{2.02} \times (N_f)^{\sqrt{2.02}}$$

Where N_i is the number of cycles to initiate the crack and N_f is the total number of cycles to failure.

(i) Determine the cyclic lifetime of two specimens, one having a N_i/N_f ratio of 0.01 corresponding to a stress range $\Delta\sigma_1$ and the other having a N_i/N_f ratio of 0.99 corresponding to a stress range $\Delta\sigma_2$.

(ii) If the crack at failure is 1 mm deep, determine the mean crack propagation rate of $\Delta\sigma_1$ and the mean crack nucleation rate at $\Delta\sigma_2$.

[103 cycles, 5.66×10^6 cycles, 9.794×10^{-3} mm/cycle, 17.83×10^{-9} mm/cycle]

11.2 (B). (a) "Under fatigue conditions it may be stated that for less than 1000 cycles, life is a function of ductility and for more than 10,000 cycles life is a function of strength." By consideration of cyclic strain-stress behaviour, show on what grounds this statement is based.

(b) In a tensile test on a steel specimen, the fracture stress was found to be 520 MN/m^2 and the reduction in area 25%.

Calculate: (i) the plastic strain amplitude to cause fracture in 100 cycles; (ii) the stress amplitude to cause fracture in 10^6 cycles. [0.0268; 173.4 MN/m^2]

11.3 (B). An aluminium cantilever beam, 0.762 m long by 0.092 m wide and 0.183 m deep, is subjected to an end downwards fluctuating load which varies from a minimum value P_{\min} of 8.9 kN to some maximum value P_{\max} .

The material has a fatigue strength for complete stress reversal σ_N of 206.7 MN/m^2 and a static yield strength σ_y of 275.6 MN/m^2 .

By consideration of the Soderberg equation, derive an expression for P_{\max} and show that it is equal to:

$$\frac{2I\sigma_N}{y(1+p)L} + \frac{(1-p)}{(1+p)}P_{\min}$$

where $p = \sigma_N/\sigma_y$ and y is the distance of the extreme fibres from the neutral axis of bending and I is the second moment of area of the beam section. Determine the minimum value of P_{\max} which will produce failure of the beam.

[159 kN]

11.4 (B). (a) Explain the meaning of the term "stress concentration" and discuss its significance in relation to the fatigue life of metallic components.

(b) A member made of steel has the size and shape indicated in Fig. 11.52.

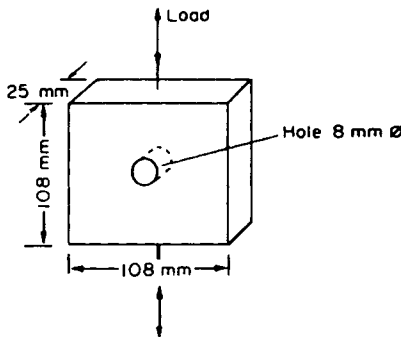


Fig. 11.52.

The member is subjected to a fluctuating axial load that varies from a minimum value of $P/2$ to a maximum value of P . Use the Soderberg equation to determine the value of P that will produce failure in 10^6 cycles.

Assume:

Yield strength of steel = 420 MN/m²

Fatigue strength of steel = 315 MN/m² for 10⁶ cycles

Notch sensitivity factor = 0.9

Static stress concentration factor = 3.0

[0.62 MN]

11.5 (B). (a). Explain briefly the concepts of survival probability and cumulative damage in respect of fatigue of structural components.

(b) The loading spectrum on an aluminium alloy component is given below for every 100 000 cycles. Also shown is the fatigue life at each stress level.

Determine an expected fatigue life based upon Miner's Hypothesis of damage.

Stress amplitude MN/m ²	Number of cycles in each 10 ⁵ cycles	Fatigue life (<i>N_f</i>)
340	3000	80 000
290	8000	330 000
240	15 000	1000 000
215	34 000	3000 000
190	40 000	35000 000

[11.21 × 10⁵ cycles]

11.6 (B). A stress analysis reveals that at a point in a steel part the stresses are $\sigma_{xx} = 105$, $\sigma_{yy} = 35$, $\sigma_{zz} = -20$, $\tau_{xy} = 56$, $\tau_{yz} = 10$, $\tau_{zx} = 25$ MN/m². These stresses are cyclic, oscillating about a mean stress of zero. The fatigue strength of the steel is 380 MN/m². Determine the safety factor against fatigue failure. Assume that the fatigue could initiate at a small internal flaw located at the point in question, and assume a stress-concentration factor of 2. Ignore the effect of triaxial stresses on fatigue. [1.35]

11.7 (B). (a) Briefly discuss how the following factors would affect the fatigue life of a component:

- (i) surface finish,
- (ii) surface treatment,
- (iii) surface shape.

(b) An aluminium airframe component was tested in the laboratory under an applied stress which varied sinusoidally about a mean stress of zero. The component failed under a stress range of 280 MN/m² after 10⁵ cycles and under a stress range of 200 MN/m² after 10⁷ cycles. Assuming that the fatigue behaviour can be represented by:

$$A\sigma(N_f)^a = C$$

where *a* and *C* are constants, find the number of cycles to failure for a component subjected to a stress range of 150 MN/m².

(c) After the component has already endured an estimated 4 × 10⁸ cycles at a stress range of 150 MN/m², it is decided that its failure life should be increased by 4 × 10⁸ cycles. Find the decrease in stress range necessary to achieve this additional life.

You may assume a simple cumulative damage law of the form:

$$\sum \frac{N_i}{N_f} = 1 \quad [15.2 \text{ MN/m}^2]$$

11.8 (B). (a) Write an account of the effect of mean stress upon the fatigue life of a metallic component. Include within your account a brief discussion of how mean stress may be allowed for in fatigue calculations.

(b) A thin-walled cylindrical vessel 160 mm internal diameter and with a wall thickness of 10 mm is subjected to an internal pressure that varies from a value of $-P/4$ to *P*. The fatigue strength of the material at 10⁸ cycles is 235 MN/m² and the tensile yield stress is 282 MN/m². Using the octahedral shear theory, determine a nominal allowable value for *P* such that failure will not take place in less than 10⁸ cycles. [36.2 MN/m²]

11.9 (B). (a) The Manson-Haferd creep parameter method was developed on an entirely empirical basis, whilst those of Larson-Miller and Skerby-Dorn are based upon the well known Arrhenius equation. Compare all three extrapolation methods and comment on the general advantages and disadvantages of applying these methods in practice.

(b) The following table was produced from the results of creep tests carried out on specimens of Nimonic 80 A.

Stress (MN/m ²)	Temperature (°C)	Time to rupture (h)
180	752	56
180	502	1000
300	452	316
300	317	3160

Use the information given to produce a master curve based upon the Manson–Haferd parameter and thus estimate the expected life of a material when subjected to a stress of 250 MN/m² and a temperature of 400°C. [1585 hours]

11.10 (B). (a) Briefly describe the generally desirable characteristics of a material for use at high temperatures.

(b) A cylindrical tube in a chemical plant is subjected to an internal pressure of 6 MN/m² which leads to a circumferential stress in the tube wall. The tube is required to withstand this stress at a temperature of 575°C for 9 years.

A designer has specified tubes of 40 mm bore and 2 mm wall thickness made from a stainless steel and the manufacturer’s specification for this alloy gives the following information at $\sigma = 200$ MN/m².

Temp (°C)	500	550	600	650	700
ϵ/S	1.0×10^{-6}	2.1×10^{-6}	4.3×10^{-6}	7.7×10^{-6}	1.4×10^{-5}

Given that the effect of stress and temperature upon creep rate can be considered by the following equation:

$$\dot{\epsilon} = A\sigma^6 e^{-\Delta H/RT}$$

and that failure of the tube will take place at a strain of 0.01, with the aid of a graph, calculate whether the tube will fulfil its design life function. [No, $\epsilon_9 = 2.07$]

11.11 (B). (a) By consideration of the Arrhenius equation, discuss the theoretical basis of the Larson–Miller parameter as applied to creep data and compare it with other well known alternative parameters.

(b) From the figures given below, determine the expected life at 650°C of an alloy steel when subjected to a stress of 205 MN/m².

Stress (MN/m ²)	Temperature (°C)	Life (h)
205	700	1000
205	720	315

[22 330 hours]

11.12 (B). A cylindrical polymer component is produced at constant pressure by expanding a smaller cylinder into a cylindrical mould. The initial polymer cylinder has length 1200 mm, internal diameter 20 mm and wall thickness 5 mm; and the mould has diameter 100 mm and length 1250 cm. Show that, neglecting end effects, the diameter of the cylindrical portion (which may be considered thin) will increase without any change of length until the material touches the mould walls. Hence determine the time taken for the plastic material to reach the mould walls under an internal pressure of 10 kN/m², if the uniaxial creep equation for the polymer is $d\epsilon/dt = 32\sigma$, where t is the time in seconds and σ is the stress in N/mm²

The Levy–von Mises equations which govern the behaviour of the polymer are of the form

$$d\epsilon_1 = \frac{d\epsilon_e}{\sigma_e} \left[\sigma_1 - \frac{1}{2}(\sigma_2 + \sigma_3) \right]$$

where σ_e is the equivalent stress and ϵ_e is the equivalent strain. [1 second]

11.13 (B). (a) Explain, briefly, the meaning and importance of the term “stress relaxation” as applied to metallic materials.

(b) A pressure vessel is used for a chemical process operating at a pressure of 1 MN/m² and a temperature of 425°C. One of the ends of the vessel has a 400 mm diameter manhole placed at its centre and the cover plate is held in position by twenty steel bolts of 25 mm diameter spaced equally around the flanges.

Tests on the bolt steel indicate that $n = 4$ and $\epsilon^\circ = 8.1 \times 10^{-10}/h$ at 21 MN/m² and 425°C. Assuming that the stress in a bolt at any time is given by the equation:

$$\frac{1}{\sigma_t^{n-1}} = \frac{1}{\sigma_i^{n-1}} + \beta E(n-1)t$$

and that the secondary creep rate can be represented by the relationship $\epsilon^\circ = \beta\sigma^n$, with E for the bolt steel = 200 GN/m², calculate:

- (i) the initial tightening stress in the bolts so that after 10 000 hours of creep relaxation there is still a safety factor of 2 against leakage,
- (ii) the total time for leakage to occur. [30.7 MN/m²; 177.2 × 10³ hours]

11.14 (B). (a) The lives of Nimonic 90 turbine blades tested under varying conditions of stress and temperature are set out in the table below:

Stress (MN/m ²)	Temperature (°C)	Life (h)
180	750	3000
180	800	500
300	700	5235
350	650	23 820

Use the information given to produce a master curve based upon the Larson–Miller parameter, and thus calculate the expected life of a blade when subjected to a stress of 250 MN/m² and a temperature of 750°C.

- (b) Discuss briefly the advantages and disadvantages of using parametric methods to predict creep data compared with the alternative method of using standard creep strain–time curves. [1365 hours]

11.15 (B). (a) A support bracket is to be made from a steel to be selected from the table below. It is important that, if overloading occurs, yielding takes place before fracture. The thickness of the section is 10 mm and the maximum possible surface crack size that could have escaped non-destructive inspection is 10% of the section thickness. Select a suitable tempering temperature from the list. Assume that this is equivalent to an edge crack in a wide plate and assume an associated flaw shape parameter of 1.05.

Tempering temperature (°C)	Yield strength (MN/m ²)	K_{IC} (MN/m ^{3/2})
480	1207	98.9
425	1413	95.4
370	1586	41.8

[425 °C]

11.16 (B). A high-speed steel circular saw of 300 mm diameter and 3.0 mm thickness has a fatigue crack of length 26 mm running in a radial direction from the spindle hole. Assume that this is an edge crack in a semi-infinite plate. The proof strength of this steel is 1725 MN/m² and its fracture toughness is 23 MN/m^{3/2}. The tangential stress component adjacent to the spindle hole during operation has been calculated as follows:

Periphery temperature relative to centre (°C)	Tangential stress (MN/m ²)
10	27
30	50
50	72

First estimate the size of the plastic zone in order to decide whether plane strain or plane stress conditions predominate. Then estimate at what periphery temperature the saw is likely to fail by fast fracture.

[0.0226 mm; 50°C]

What relative safety factor (on tangential stress) can be gained by using a carbide-tipped lower-strength but tougher steel saw of yield strength 1200 MN/m² and fracture toughness 99 MN/m^{3/2}, in the case of the same size of fatigue crack? [4.3]

11.17 (B). (a) When a photoelastic model similar to the one shown in Fig. 11.39 is stressed the fifth fringe is found to have a maximum distance of 2.2 mm from the crack tip. If the fringe constant is 11 N/mm²/fringe-mm

and the model thickness is 5 mm, determine the value of the stress-intensity factor (in $\text{N/m}^{3/2}$) under this applied load. Discuss any important errors which could be associated with this measurement. [1.293 $\text{MN/m}^{3/2}$]

(b) Suggest a way of checking to ensure that the stresses are purely mode I (i.e. those tending to “open” the crack) and that there is no superimposed mode II component (i.e. the tendency to shear the crack along its plane, as shown in Figure 11.34).

11.18 (B). (a) The stresses near the crack tip of a specimen containing a through-thickness crack loaded in tension perpendicular to the crack plane are given by the following equations

$$\sigma_{xx} = \frac{K_I \cos \frac{\theta}{2}}{\sqrt{2\pi r}} \left[1 - \sin \frac{\theta}{2} \cdot \sin \frac{3\theta}{2} \right]$$

$$\sigma_{yy} = \frac{K_I \cos \frac{\theta}{2}}{\sqrt{2\pi r}} \left[1 + \sin \frac{\theta}{2} \cdot \sin \frac{3\theta}{2} \right]$$

$$\sigma_{xy} = \frac{K_I \cos \frac{\theta}{2}}{\sqrt{2\pi r}} \left[\sin \frac{\theta}{2} \cdot \cos \frac{3\theta}{2} \right]$$

where K_I is the stress intensity factor, r is the distance from the crack tip and θ is the angle measured from the projected line of the crack in the uncracked region.

Using the proportions of Mohr’s circle, or otherwise, show that the maximum shear stress near the crack tip is given by:

$$\tau_{\max} = \frac{K_I \sin \theta}{2\sqrt{2\pi r}}$$

(b) Sketch the photoelastic fringe pattern which would be expected from a model of this loading case.

(c) In such a fringe pattern the fourth fringe occurs at a distance of 1.45 mm from the crack tip. If the material fringe constant is 10.5 $\text{kN/m}^2/\text{fringe/m}$ and the model thickness is 5 mm determine the value of K_I under the given applied load. What error is associated with this measurement? [0.8 $\text{MN/m}^{3/2}$]

11.19 (B). (a) Write a short essay on the application of fracture mechanics to the problem of crack growth in components subjected to alternating loading conditions.

(b) After two years service a wide panel of an aluminium alloy was found to contain a 5 mm long edge crack orientated normal to the applied stress. The panel was designed to withstand one start-up/shut-down cycle per day for 20 years (assume 250 operating days in a year), the cyclic stress range being 0 to 70 MN/m^2 .

If the fracture toughness of the alloy is 35 $\text{MNm}^{-3/2}$ and the cyclic growth rate of the crack is represented by the equation:

$$\frac{da}{dN} = 3.3 \times 10^{-9} (\Delta K)^{3.0}.$$

calculate whether the panel will meet its design life expectancy. (Assume $K_I = \sigma\sqrt{\pi a}$).

[No – 15.45 years]

11.20 (B). (a) Differentiate between the terms “stress concentration factor” and “stress intensity factor”.

(b) A cylindrical pressure vessel of 7.5 m diameter and 40 mm wall thickness is to operate at a working pressure of 5.1 MN/m^2 . The design assumes that failure will take place by fast fracture from a crack and to prevent this the total number of loading cycles must not exceed 3000.

The fracture toughness of the sheet is 200 $\text{MNm}^{3/2}$ and the growth of the crack may be represented by the equation:

$$\frac{da}{dN} = A(\Delta K)^4$$

Where $A = 2.44 \times 10^{-14}$ and K is the stress intensity factor. Find the minimum pressure to which the vessel must be tested before use to guarantee against fracture in under 3000 cycles. [8.97 MN/m^2]

11.21 (B). (a) Write a short essay on application of fracture mechanics to the problem of crack growth in components subjected to alternating loading conditions.

(b) Connecting rods for an engine are to be made of S.G. iron for which $K_{IC} = 25 \text{MNm}^{-3/2}$. NDT will detect cracks or flaws of length $2a$ greater than 2 mm, and rods with flaws larger than this are rejected.

Independent tests on the material show that cracks grow at a rate such that

$$da/dN = 2 \times 10^{-15} (\Delta K_I)^3 \text{ m cycle}^{-1}$$

The minimum cross-sectional area of the rod is 0.01 m^2 , its section is circular and the maximum tensile load in service is 1 MN.

Assuming that $K_I = \sigma\sqrt{\pi a}$ and the engine runs at 1000 rev/min calculate whether the engine will meet its design requirement of 20,000 h life. [$N_f = 4.405 \times 10^9$ and engine will survive]

11.22 (B). (a) By considering constant load conditions applied to a thin semi-infinite sheet and also the elastic energy in the material surrounding an internal crack of unit width and length $2c$, derive an expression for the stress when the crack propagates spontaneously.

(b) A pipeline is made from a steel of Young's modulus $2.06 \times 10^{11} \text{ Nm}^{-2}$ and surface energy 1.1 J m^{-2} .

Calculate the critical half-length of a Griffith crack for a stress of $6.2 \times 10^6 \text{ Nm}^{-2}$, assuming that all the supplied energy is used for forming the fracture surface.

$$\left[\sqrt{\frac{2\gamma E'}{\pi c}}, 3.752 \text{ mm} \right]$$

11.23 (B). (a) Outline a method for determining the plane strain fracture toughness K_{IC} , indicating any criteria to be met in proving the result valid.

(b) For a standard tension test piece, the stress intensity factor K_I is given by:

$$K_I = \frac{P}{BW^{1/2}} \left[29.6 \left(\frac{a}{W} \right)^{1/2} - 32.04 \left(\frac{a}{W} \right)^{3/2} \right]$$

the symbols having their usual meaning.

Using the DC potential drop crack detection procedure the load at crack initiation P was found to be 14.6 kN. Calculate K_{IC} for the specimen if $B = 25 \text{ mm}$, $W = 50 \text{ mm}$ and $a = 25 \text{ mm}$.

(c) If $\sigma_1 = 340 \text{ MN/m}^2$, calculate the minimum thickness of specimen which could be used still to give a valid K_{IC} value. [$25.07 \text{ MNm}^{-3/2}$, 13.6 mm]